Functional genomics reveals the mechanism of hypoxic adaptation in nontuberculous mycobacteria

Yoshitaka Tateishi[1*], Yuriko Ozeki[1], Akihito Nishiyama[1], Yuta Morishige[2], Yusuke Minato[3,4], Anthony D. Baughn[4], Sohkichi Matsumoto[1,5]

1. Department of Bacteriology, Graduate School of Medicine and Dental Sciences, Niigata University, 1-757, Asahimachi-dori, Chuo-ku, Niigata 951-8510, Japan.
2. Department of Mycobacterium Reference and Research, Research Institute of Tuberculosis, Japan Anti-Tuberculosis Association, Kiyose, Tokyo, 2048533, Japan.
3. Department of Microbiology, Fujita Health University School of Medicine, Toyoake, Aichi, Japan.
4. Department of Microbiology and Immunology, University of Minnesota Medical School, 689 23rd Avenue S.E. Microbiology Research Facility, Minneapolis, 55455, MN, USA.
5. Laboratory of Tuberculosis, Institute of Tropical Disease, Universitas Airlangga, Surabaya, East Java, Indonesia.

e-mail: y-tateishi@med.niigata-u.ac.jp

Abstract

Mycobacterium intracellulare is a major etiological agent of the recently expanding *Mycobacterium avium–intracellulare* complex pulmonary disease (MAC-PD). Therapeutic regimens that include a combination of macrolides and antituberculous drugs have been implemented with limited success. To identify novel targets for drug development that accommodate the genomic diversity of *M. avium–intracellulare*, we subjected eight clinical MAC-PD isolates and the type strain ATCC13950 to genome-wide profiling to comprehensively identify universally essential functions. Among these strains, we identified 131 shared essential or growth-defect-associated genes. Unlike the type strain, the clinical strains showed an increased requirement for genes involved in gluconeogenesis and the type VII secretion system under standard growth conditions, the same genes required for hypoxic pellicle-type biofilm formation in ATCC13950. Consistent with the central role of hypoxia in the evolution of *M. intracellulare*, the clinical MAC-PD strains showed more rapid adaptation to hypoxic growth than the type strain. Importantly, the increased essentiality of hypoxic fitness genes was confirmed in a mouse lung infection model. These findings confirm the concordant gene essentiality under hypoxic conditions *in vitro* and hypoxia-related conditions *in vivo*, and highlight

37 the importance of using clinical strains and host-relevant growth conditions to identify

38 high-value targets for drug development.

39

40 **Introduction**

41 In contrast to the ongoing decline in the rate of tuberculosis, *Mycobacterium avium–*

42 *intracellulare* complex pulmonary disease (MAC-PD) is increasing in many parts of the

43 world[1,2]. The standard therapy for MAC-PD involves multidrug chemotherapy that

44 includes clarithromycin and several antituberculous drugs. Unfortunately, treatment

45 failure is common, resulting in relapse, disease progression, and death[3]. Therefore, it is

46 critical to investigate the bacterial physiological characteristics that underlie the ability

47 of MAC-PD strains to establish and maintain chronic drug-recalcitrant infections.

48 Recent advances in comparative genomics have revealed major differences in

49 the genomic features of reference type strains and circulating pathogenic clinical

50 isolates. Extensive genomic diversity has been recognized across clinical isolates of

51 nontuberculous mycobacteria (NTM). *Mycobacterium avium* has been divided into four

52 subspecies including subspecies, *avium*, *hominissuis*, *silvaticum*, and *paratuberculosis* [4].

53 Whereas *M. intracellulare* has been divided into two subgroups, typical *M.*

54 *intracellulare* (TMI) and *M. paraintracellulare–M. indicus pranii* (MP-MIP), with

55 currently two additional distinguished subspecies, *yongonense*, and *chimaera*[5,6]. Despite
56 the increasing number of sequenced MAC-PD strains, the molecular genetic
57 mechanisms that underlie their virulence and pathogenesis are still poorly understood.
58 The burgeoning field of functional genomics has allowed the rapid assessment
59 of molecular aspects of organisms on a genome-wide scale. Transposon (Tn) sequencing
60 (TnSeq) is a functional genomic approach that combines saturation-level transposon-
61 insertion mutagenesis with next-generation sequencing (NGS) to comprehensively
62 evaluate the fitness costs associated with gene inactivation in bacteria. Over the last
63 decade, TnSeq has been applied to numerous bacterial species using various
64 approaches[7]. Whereas initial studies applied TnSeq to reference strains, recent
65 approaches have included the comparative assessment of representative clinical strains
66 to better understand the fundamental aspects of pathogen biology[8]. We have previously
67 used TnSeq to globally characterize the genes that are essential for growth versus those
68 that are essential for hypoxic pellicle formation in the *M. intracellulare* type strain
69 ATCC13950[9]. However, given the recent expansion of MAC-PD and the well-
70 recognized high levels of genomic diversity in this complex of bacteria, data obtained
71 from the study of a decades-old reference strain is not expected to represent the
72 diversity of extant clinical isolates. ATCC13950 was originally isolated from the

73 abdominal lymph node of the 34-month-old female[10]. Even though the etiological
74 bacterial species are the same, the clinical manifestation of infant lymphadenitis differs
75 markedly from MAC-PD, which often occurs in middle-aged and elderly female
76 patients with no predisposing immunological disorder. Therefore, it is essential to
77 investigate a collection of strains that captures the diversity of recent clinical MAC-PD
78 strains in order to define key molecular aspects of their pathogenesis and virulence.
79 In this study, we used TnSeq to analyze a set of recently isolated clinical *M.*
80 *intracellulare* strains with diverse genotypes. We integrated the gene essentiality data
81 for these strains and the type strain to identify the common essential and growth-defect-
82 associated genes that represent the genomic diversity of this group of pathogens. We
83 also identified the greater essentiality of genes involved in gluconeogenesis, the type
84 VII secretion system, and cysteine desulfurase in the clinical MAC-PD strains than in
85 the type strain. Furthermore, the requirement for these genes was confirmed in a mouse
86 lung infection model. The profiles of gene essentiality in clinical MAC-PD strains
87 suggest the mechanism of hypoxic adaptation in NTM in terms of promising drug
88 targets, especially for strains that cause clinical MAC-PD.
89
90 **Results**

91 **Common essential and growth-defect-associated genes representing the genomic**

92 **diversity of *M. intracellulare* strains**

93 To obtain comprehensive information on the genome-wide gene essentiality of *M.*

94 *intracellulare*, we included nine representative strains of *M. intracellulare* with diverse

95 genotypes in this study (Fig. 1a, b). We used TRANSIT[11] to obtain 2–6 million reads of

96 Tn insertions. The average number of Tn insertion reads was > 50 at Tn-inserted TA

97 sites, which confirmed the TnSeq data (Supplementary Table 1). The numbers of

98 essential genes in the clinical MAC-PD strains, calculated with the hidden Markov

99 model (HMM; a transition probability model), tended to be smaller than that in

100 ATCC13950 (Supplementary Table 2). In total, 131 genes were identified as essential or

101 growth-defect-associated with the HMM analysis across all *M. intracellulare* strains,

102 including the eight MAC-PD clinical strains and ATCC13950 (Fig. 2a, Supplementary

103 Table 3). The genes identified as universal essential or growth-defect-associated were

104 involved in fundamental functions, such as glyoxylate metabolism, purine/pyrimidine

105 metabolism, amino acid synthesis, lipid biosynthesis, arabinogalactan/peptidoglycan

106 biosynthesis, porphyrin metabolism, DNA replication, transcription, amino acid tRNA

107 ligases, ribosomal proteins, general secretion proteins, components of iron–sulfur

108 cluster assembly, some ABC transporters, and the type VII secretion system. The genes

109 identified corresponded to the genes that encode conventional and under-development
110 drug targets, such as those encoding gyrase, arabinosyltransferase, enoyl-(acyl-carrier-
111 protein) reductase, alanine racemase, DNA-directed RNA polymerase, malate
112 synthase[12] and F_0F_1 ATP synthase (Fig. 2b). These data suggest that the set of universal
113 essential or growth-defect-associated genes identified with the HMM analysis of *M.*
114 *intracellulare* strains with diverse genotypes has potential utility as antibiotic drug
115 targets.

116 By comparative genomic analysis, we have revealed 3,153 core genes among
117 55 *M. intracellulare* strains including those used in this study[5]. Of these core genes, 439
118 genes were classified as strain-dependent essential or growth-defect-associated with the
119 HMM analysis (Supplementary Table 4). And among 5,824 accessory genes, 222 genes
120 were classified as essential or growth-defect-associated with the HMM analysis. The
121 proportion of these strain-dependent and accessory essential or growth-defect-associated
122 genes was comparable to the similar analysis of *Streptococcus pneumoniae*[13]. Of note,
123 17 (3.8%) of strain-dependent essential or growth-defect-associated genes and 14
124 (6.3%) of accessory essential or growth-defect-associated genes were also included in
125 the 175 genes required for hypoxic pellicle formation in ATCC13950 reported in our
126 previous study[9] (Supplementary Table 4).

127

128 **Genes with increased gene essentiality in clinical MAC-PD strains are also**

129 **required for hypoxic pellicle formation in the type strain**

130 The sharing of strain-dependent and accessory essential or growth-defect-associated

131 genes with genes required for hypoxic pellicle formation in ATCC13950 prompts us to

132 consider the possibility that the clinical MAC-PD strains increase the gene essentiality

133 of the genes involved in hypoxic growth compared to ATCC13950. To clarify this, we

134 compared the gene essentiality of the clinical MAC-PD strains with that in ATCC13950

135 by integrating the HMM analysis with the resampling analysis, a method of calculating

136 the number of significantly altered Tn insertion reads (a gene-based permutation

137 model). With this integrating analysis, 121 genes in the clinical MAC-PD strains were

138 shown to have significantly fewer Tn insertions than ATCC13950 (Fig. 3,

139 Supplementary Tables 5, 6). Of these, nine genes were identified in 3–5 clinical MAC-

140 PD strains. These included genes encoding phosphatases (OCU_RS30185,

141 OCU_RS35795), cysteine desulfurase (*csd* [OCU_RS40305]), methyl transferase

142 (OCU_RS41540), a hypothetical protein (OCU_RS47290), type VII secretion

143 components (*mycP5* [OCU_RS38275], *eccC5* [OCU_RS38345]), a glycine cleavage

144 system aminomethyltransferase (*gcvT* [OCU_RS35955]), and phosphoenolpyruvate

145 carboxykinase (*pckA* [OCU_RS48660]) (Figs 3, 4). The genes involved in
146 gluconeogenesis (such as *pckA*), the glycine cleavage system, and the type VII secretion
147 system were also identified as required for hypoxic pellicle formation in ATCC13950 in
148 our previous study[9]. The Tn insertion reads were significantly reduced in the pathways
149 of gluconeogenesis, including in fructose-1,6-bisphosphatase (*glpX*),
150 phosphoenolpyruvate carboxykinase (*pckA*), and pyruvate carboxylase (*pca*), but were
151 significantly increased in those of glycolysis, including in pyruvate kinase (*pykA*) and
152 pyruvate dehydrogenase (*aceE*, *lpdC*), suggesting that carbohydrate metabolism was
153 metabolically remodeled in the clinical MAC-PD strains, which mimics the metabolism
154 observed during hypoxic pellicle formation in ATCC13950 (Fig. 5).
155 On the other hand, 162 genes were detected with significantly more Tn insertions in
156 the clinical MAC-PD strains than in ATCC13950 (Fig. 3). Of these, 12 genes were
157 identified in more than seven strains. The increased Tn insertion reads in the genes
158 encoding superoxide dismutase (OCU_RS25945) and pyruvate dehydrogenase (*aceE*
159 [OCU_RS35720]) in the clinical MAC-PD strains suggest the inessentiality of the
160 detoxification of oxygen radicals and glycolysis metabolism in these strains (Figs 3–5).
161 These genes also included those encoding amidohydrolases (OCU_RS34400,
162 OCU_RS34425, OCU_RS34445), some transcription factors (OCU_RS28440,

163 OCU_RS30230), a CoA transferase (OCU_RS34390), and some predicted transporters
164 (OCU_RS28435, OCU_RS39950, OCU_RS39955, OCU_RS44685). Furthermore, the
165 increase in Tn insertion reads in predicted multidrug-resistant genes, such as those
166 encoding the DrrAB-ABC transporter complex (OCU_RS39950, OCU_RS39955)[14] and
167 a putative lipoprotein LpqB (OCU_RS44685), encoded by the two-component system
168 *mtrAB* operon[15-16], in the clinical MAC-PD strains were found.
169
170 **Requirement of genes with increased gene essentiality in the clinical MAC-PD**
171 **strains for mouse lung infection**
172 Hypoxia is the major environmental condition in natural water[17], biofilms[18], and
173 infections in humans and animals characterized by caseous granuloma lesions[19]. The
174 impact of hypoxia on mycobacteria under various ecological circumstances implies that
175 the genes with increased essentiality in the clinical MAC-PD strains compared to
176 ATCC13950 and the genes required for hypoxic pellicle formation in ATCC13950 may
177 be required for infection *in vivo*. To examine whether the set of genes with increased
178 essentiality in the clinical MAC-PD strains also shows increased essentiality during
179 infection *in vivo*, we performed TnSeq in mice infected intratracheally with the Tn
180 mutant library strains of M.i.198 or M.i.27, which we had demonstrated to be virulent in

181 mice (Supplementary Fig. 1a). The time course of the changes in the bacterial burden
182 showed a pattern similar to those of the wild-type strains M.i.198 and M.i.27,
183 respectively, except that it was not possible to harvest sufficient colonies (as few as
184 10^4/mouse) in the few mice infected with the M.i.27 Tn mutant strain in week 8 and
185 week 16 (Supplementary Fig. 1b, Supplementary Table 7). With a resampling analysis,
186 629 and 512 genes were shown to be required for *in vivo* infection with transposon
187 mutant library strains M.i.27 and M.i.198, respectively, between day 1 and week 16 of
188 infection (Fig. 6a, Supplementary Fig. 1c, d, Supplementary Tables 8, 9). Of these
189 genes, 72 (11.9%) and 50 (9.76%) in M.i.27 and M.i.198, respectively, were also
190 required for hypoxic pellicle formation in ATCC13950. Forty-one genes also required
191 for hypoxic pellicle formation in ATCC13950 were identified in both M.i.27 and
192 M.i.198, and included genes associated with succinate production (multifunctional 2-
193 oxoglutarate metabolism enzyme) and the glyoxylate cycle (isocitrate lyase), cysteine
194 and methionine synthesis (thiosulfate sulfurtransferase [CysA], 5-
195 methyltetrahydrofolate-homocysteine methyltransferase [MetH]), the serine/threonine-
196 protein kinase PknG system, proteasome subunits (PrcA, PrcB), DNA repair UvrC,
197 secretion protein EspR, cell-wall synthesis proteins (such as phosphatidylinositol
198 [polyprenol-phosphate-mannose-dependent alpha-[1-2]-phosphatidylinositol

199 pentamannoside mannosyltransferase], peptidoglycan (penicillin-binding protein A

200 pbpA), and L,D-transpeptidase 2), putative membrane proteins and transporters (such as

201 the MmpL family, transport accessory protein MmpS3, transport protein MmpL11,

202 vitamin B_{12} transport ATP-binding protein BacA, ABC transporter substrate-binding

203 protein, and ABC transporter permease), and mammalian cell entry (Mce) proteins

204 (OCU_RS48855–48875) (Supplementary Table 10).

205 The genes only identified in M.i.27 that were also required for hypoxic pellicle

206 formation in ATCC13950 included genes associated with gluconeogenesis (*pckA*, *glpX*),

207 the glycine cleavage system (*gcvT*), the type VII secretion system (*eccD5, espG5,*

208 *eccC5* [OCU_RS38280-OCU_RS38285-OCU_RS38345], *eccC3* [OCU_RS48145]),

209 and D-inositol 3-phosphate glycosyltransferase (Supplementary Table 10). These three

210 systems, gluconeogenesis, the glycine cleavage system, and the type VII secretion

211 system, also showed increased gene essentiality in 3–5 clinical MAC-PD strains than in

212 ATCC13950 (Figs 3, 6). Although M.i.27 was excluded as a relevant strain showing

213 increased gene essentiality of these three metabolic systems, the increase in gene

214 requirements for infection *in vivo* suggests a positive relationship between hypoxic

215 growth *in vitro* and bacterial growth *in vivo*. In contrast, M.i.198 already showed

216 increased gene essentiality in these three metabolic systems under aerobic conditions *in*

217 *vitro*, so the genes associated with these three systems were not identified as having
218 fewer Tn insertion reads during infection *in vivo*. Genes only identified in M.i.198 and
219 required for hypoxic pellicle formation in ATCC13950 included genes associated with
220 succinate synthesis (2-oxoglutarate oxidoreductase subunit KorA) or encoding the
221 HTH-type transcriptional repressor KstR and menaquinone reductase (Supplementary
222 Table 10). As increased gene essentiality in 3–5 clinical strains (excluding M.i.198)
223 compared with ATCC13950, an increased requirement for the RNA methyltransferase
224 OCU_RS41540 was identified in M.i.198 during infection *in vivo*. Despite the
225 differences in the profiles of the genes required for *in vivo* infection between strains,
226 these data suggest that increased gene essentiality for hypoxic growth confers
227 advantages for pathogenesis *in vivo*.

228 We have performed a statistical enrichment analysis of gene sets by GSEA[20] to
229 investigate whether the genes required for growth of M.i.27 and M.i.198 in mouse lungs
230 overlap the gene sets required for hypoxic pellicle formation in ATCC13950 as well as
231 the gene sets showing increased gene essentiality observed in the clinical MAC-PD
232 strains listed in Fig 3. Of these gene sets including a total of 180 genes, 54% (98 genes)
233 and 40% (73 genes) were listed as enriched in genes required for mouse infection in
234 M.i.27 and M.i.198, respectively ($P < 0.01$ in M.i.27 and $P = 0.016$ in M.i.198)

235 (Supplementary Fig. 2, Supplementary Table 11). The enriched genes both in M.i.27 and
236 M.i.198 included genes encoding fructose -1,6-bisphosphatase (*glpX*), a type VII
237 secretion protein (*eccC5*), glycine cleavage system aminomethyltransferase (*gcvT*),
238 some phosphatase (OCU_RS30185) and a hypothetical protein (OCU_RS47290) (Fig.
239 6). The enriched genes only in M.i.27 included genes of phosphoenolpyruvate
240 carboxylinase (*pckA*), cysteine desulfurase (*csd*) and the ESX-5 type VII secretion
241 component serine protease (*mycP5*). The enriched genes only in M.i.198 included genes
242 encoding some phosphatase (OCU_RS35975) and class I SAM-dependent RNA
243 methyltransferase (OCU_RS41540). These data suggest the sharing of the hypoxia-
244 adaptation pathways between *in vitro* hypoxic pellicle formation and *in vivo* bacterial
245 growth.
246
247 **Preferential hypoxic adaptation of clinical MAC-PD strains evaluated with**
248 **bacterial growth kinetics**
249 The metabolic remodeling, such as the increased gene essentiality of gluconeogenesis
250 and the type VII secretion system, and the overlap of the genes required for mouse lung
251 infection and those required for hypoxic pellicle formation involved by confer these
252 metabolic pathways suggests the preferential adaptation of the clinical MAC-PD strains

253 to hypoxic conditions. To confirm this, we investigated the growth kinetics of each
254 strain under aerobic and hypoxic conditions. In terms of growth kinetics, most of the
255 clinical MAC-PD strains (except M001) entered logarithmic (log) phase earlier than
256 ATCC13950 under 5% oxygen (Fig. 7a, Supplementary Fig. 3). However, under aerobic
257 conditions, the clinical MAC-PD strains entered log phase at a similar time to
258 ATCC13950. The growth rate at mid-log point (midpoint) was significantly reduced
259 under hypoxic conditions in a total of 5 clinical MAC-PD strains (M.i.198, M.i.27,
260 M003, M019 and M021) compared to aerobic conditions (Fig. 7b, Supplementary Fig.
261 3). The growth rate at midpoint under hypoxic conditions was significantly lower in
262 these 5 clinical MAC-PD strains than in ATCC13950. By contrast, the growth rate at
263 midpoint was significantly increased under hypoxic conditions compared to aerobic
264 conditions in ATCC13950. And there was no significant change in the growth rate
265 between aerobic and hypoxic conditions in the rest 3 clinical MAC-PD strains (M018,
266 M001 and MOTT64). The data of more rapid adaptation to hypoxia followed by
267 reduced growth rate once adapted indicate the greater metabolic advantage on
268 continuous logarithmic bacterial growth under hypoxic conditions in the clinical MAC-
269 PD strains than in ATCC13950.
270

271 **Effects of knockdown of universal and accessory/strain-dependent essential or**

272 **growth-defect-associate genes in clinical MAC-PD strains**

273 To facilitate the functional analysis of the TnSeq-hit genes, it is necessary to construct

274 the genetically-engineered strains. Still now, there are very few reports of gene

275 engineering of MAC strains and none of them has been accompanied by the follow-up

276 studies[21-26]. Moreover, no attempts have been reported to construct the knockdown

277 strains in MAC strains. With an intention to break through this current situation, we

278 used the pRH2052/pRH2521 clustered regularly interspaced short palindromic repeats

279 interference (CRISPR-i) system to construct knockdown strains where the expression of

280 the target gene is suppressed[27]. Of the nine *M. intracellulare* strains analyzed in this

281 study, seven could be transformed with the vectors for single guide RNA (sgRNA)

282 expression and dCas9 expression. However, the other two strains, M001 and MOTT64,

283 could not be transformed with these CRISPR-i vectors. To confirm the gene essentiality

284 detected with the HMM analysis, we evaluated the consequent growth inhibition in the

285 knockdown strains of representative universal essential or growth-defect-associated

286 genes, including *glcB*, *inhA*, *gyrB*, and *embB*. The knockdown strains showed growth

287 suppression with comparative growth rates of knockdown strains to vector control

288 strains that do not express single sgRNA reaching 10^{-1} to 10^{-4} (Fig. 8a).

289 As representative accessory and strain-dependent essential or growth-defect-
290 associated genes, we evaluated the 9 genes showing reduced Tn insertion reads in the 3–
291 5 clinical MAC-PD strains as listed in Fig. 3, as well as *glpX*, a gene of gluconeogenesis
292 where four MAC-PD strains showed reduced Tn insertion reads in a resampling analysis
293 (Fig. 5b). The growth was suppressed in the *pckA*-knockdown strains in M.i.198 and
294 M003, in the *glpX*-knockdown strain in M003, and in the cysteine desulfurase gene
295 (*csd*)-knockdown strains in M.i.198 and M003, with comparative growth rates of
296 knockdown strains to vector control strains reaching 10^{-2} to 10^{-4} (Fig. 8b). The growth
297 tended to be suppressed in the type VII secretion protein gene (*eccC5*)-knockdown
298 strain in M003 and in the type VII secretion-associated serine protease mycosin gene
299 (*mycP5*)-knockdown strain in M003, with comparative growth rates of knockdown
300 strains to vector control strains reaching less than 10^{-1}. By contrast, the growth was not
301 suppressed in these knockdowns trains in ATCC13950, with comparative growth rates
302 of knockdown strains to vector control strains not reaching 10^{-1}, which was consistent to
303 the inessentiality of these genes under aerobic conditions in ATCC13950. As for
304 M.i.198 and M003, the consistency between TnSeq data and CRISPR-i data was
305 supported by a correlation between the growth suppression of the knockdown strains
306 and the fitness costs evaluated by a resampling analysis (Supplementary Table 12).

307 In contrast to the cases of M.i.198 and M003, the growth of knockdown strains
308 of the accessory and strain-dependent essential genes was not effectively suppressed in
309 the other MAC-PD strains despite positively detected in TnSeq (Fig. 5b, Supplementary
310 Fig. 4). These data suggest the difficulties in the effective operation of genetically
311 modified system using foreign genes from different bacterial species in MAC-PD
312 strains. Although the suppression of gene expression was confirmed in the knockdown
313 strains of these accessory and strain-dependent essential or growth-defect-associate
314 genes, the gene expression levels were not suppressed to < 1% as reported in *M.*
315 *tuberculosis* (Mtb)[28] (Supplementary Fig. 5). The differences between strains as well as
316 between genes in the degree of suppression of gene expression required to inhibit
317 bacterial growth may explain such inconsistencies between the TnSeq and CRISPR-i
318 data.
319 To be summarized, we could validate the universal essential or growth-defect-
320 associated genes by the CRISPR-i system in the *M. intracellulare* strains used in this
321 study. And, although not successful with all strains, we could validate the accessory and
322 strain-dependent essential or growth-defect-associated genes, especially genes of
323 gluconeogenesis, type VII secretion components and iron-sulfur cluster assembly in
324 several MAC-PD strains like M.i.198 and M003.

325

326 **Discussion**

327 In this study, using TnSeq of nine genetically diverse *M. intracellulare* strains, we have
328 identified 131 shared essential and growth-defect-associated genes with an HMM
329 analysis. The genes identified are promising drug targets, representing the genomic
330 diversity of the clinical MAC-PD strains and reflecting the actual clinical situation. The
331 strategy of narrowing the essential genes of bacteria is a useful approach for refining the
332 database of drug targets. We have also demonstrated an overview of the differences in
333 gene essentiality required for hypoxic growth between the ATCC type strain and the
334 clinical *M. intracellulare* strains responsible for MAC-PD, with the evidence of earlier
335 entry to log phase followed by slower growth rate observed in most of these clinical
336 strains compared to ATCC13950. This is the first study to demonstrate the positive
337 relationship between the profiles of increased gene essentiality required for hypoxic
338 metabolic remodeling and the phenotypes advantageous for bacterial survival under
339 hypoxic conditions.

340 In this study, 121 genes were detected as significantly reduced Tn insertion in the
341 clinical MAC-PD strains compared to ATCC13950, which was higher than the case of
342 Mtb showing 10–50 genes with altered Tn insertion reads detected by a resampling

343 analysis[8]. This may reflect the genomic diversity of *M. intracellulare* compared with
344 that of Mtb. The proportion of accessory genes is larger in NTM than in Mtb[29]. In a
345 clinical trial of phage therapy for *M. abscessus* infection, the number of accessory genes
346 was shown to decrease with the loss of virulence in *M. abscessus* during the course of
347 therapy[30], suggesting some role for accessory genes for its clinical pathogenesis. Our
348 data of the overlap of the accessory essential or growth-defect-associated genes such as
349 *pckA* and *mycP5* (Supplementary Table 5) with genes required for mouse lung infection
350 (Fig. 6b, Supplementary Fig. 2) supports the idea that accessory genes (non-core genes)
351 may encode functions required for bacterial survival, especially under nonoptimal
352 conditions, such as hypoxia and during the infection of human and animal bodies.
353 Our TnSeq data are consistent with metabolomic data that have shown the
354 importance of the gluconeogenic carbon flow of TCA cycle intermediates for bacterial
355 growth under hypoxic conditions in terms of the essentiality of PckA and the reverse
356 TCA cycle[31–34]. Gluconeogenesis is essential for bacterial growth when fatty acids are
357 used as a major nutrient[33]. PckA catalyzes the conversion of the metabolites derived
358 from the TCA cycle to the metabolites of gluconeogenesis[32]. The reaction catalyzed by
359 PckA is essential for bacterial growth when the available nutrients are predominantly
360 fatty acids[35,36]. The main nutrients for mycobacteria inside hypoxic granulomas in an

361 infected human or mouse body are lipids, such as fatty acids and cholesterol, rather than
362 carbohydrates[33,37]. In the present study, *M. intracellulare* grew under 5% oxygen,
363 whereas Mtb stops growing under 1% oxygen and enters a dormant state[32]. The
364 depletion of phosphoenolpyruvate in the *pckA* deletion mutant of Mtb reduced the
365 phosphoenolpyruvate–carbon flux essential for bacterial growth and drug sensitivity[32].
366 The present study supports the idea that PckA is essential for the microaerobic growth
367 of mycobacteria. Our TnSeq data imply the preferential adaptation of the clinical MAC-
368 PD strains for circumstances *in vivo*, which are characterized by hypoxia.
369 On the other hand, such metabolic shift towards gluconeogenesis and reverse TCA
370 cycle can also be observed under reactive nitrogen specie and *in vivo* infection as well.
371 This suggests that the metabolic shift observed under hypoxia is a general stress
372 response rather than being specific to hypoxia due to the nature of the
373 provided/available carbon source[38]. Several factors other than hypoxia can be estimated
374 to be related to the change of the gene essentiality in the clinical MAC-PD strains such
375 as host-related factors and general stress conditions (i.e. nutrition of abundant fatty
376 acids and less carbohydrates, low pH circumstances)[33,35-37]. Except for our data of the
377 profile of genes required for hypoxic pellicle formation in *M. intracellulare*[9], no
378 fundamental genome-wide data are available on the change of the gene essentiality in

379 response to each stress factors in non-tuberculous mycobacteria. Further studies are
380 needed to discriminate which factors are specifically involved in the increased
381 essentiality of each gene. Although of interest, it is beyond the scope of the current
382 study.

383 About 10% of the genes required for mouse infection are also required for hypoxic
384 pellicle formation. The genes showing increased gene essentiality in the clinical MAC-
385 PD strains, such as *pckA* and genes encoding the ESX-5 type VII secretion system,
386 including *eccC5* and *mycP5*, also showed increased gene requirements in mouse
387 infections. In a TnSeq study of mice infected intravenously with *M. avium*, the genes of
388 the ESX-5 type VII secretion system were required for infection of the liver and
389 spleen[39]. The ESX-5 type VII secretion system is involved in the transport of fatty acids
390 and the virulence of mycobacteria[40,41]. These similarities in the profiles of gene
391 essentiality prompt us to propose some role of biofilm formation in mycobacterial
392 pathogenesis in animals and humans. In the present study, we shed light on the impact
393 of hypoxia on biofilm formation, the acquisition of virulence, and the *in vivo*
394 pathogenesis of NTM in terms of global gene essentiality. Although the morphologies of
395 the pellicle and macroscopic lesions (including cavitation and nodular bronchiectasis)
396 are not similar, monitoring the expression of the genes identified in this study may

397 provide clues to the mechanism of biofilm formation *in vivo*.

398 In this study, we revealed the pattern of hypoxic adaptation characteristic to the
399 clinical MAC-PD strains by the growth curve analysis: an early entry to log phase
400 followed by a reduced growth rate (Fig. 7). This pattern implicates the continuous impact
401 on the infected hosts during logarithmic bacterial growth, which may be involved in the
402 persistent and steadily progressive illness for years in humans[3]. The advantage of slow
403 growth in mycobacteria may be inferred by the role of a histone-like nucleoid protein,
404 Mycobacterial DNA-binding protein 1 (MDP1), also designated HupB[42-44]. The
405 expression of MDP1 is enhanced in the stationary phase, resulting in reduced growth
406 speed and long-term survival with increased resistance to reactive oxygen species
407 (ROS)[42-44]. The reduced growth rate after entry to log phase may allow long-term survival
408 of mycobacteria under ROS-rich circumstances inside host cells. The pattern of hypoxic
409 adaptation as observed in the clinical MAC-PD strains may enhance the pathogenesis by
410 extending the period of the repeated process of bacterial invasion and replication in
411 infected macrophages.

412 Contrary to our expectation, not all clinical strains showed rapid adaptation from
413 aerobic to hypoxic conditions relative to ATCC13950. These data suggest that some, but
414 not a major proportion of, clinical *M. intracellulare* strains do not have an advantageous

415 phenotype for continuous logarithmic growth under hypoxia. In Mtb, the adaptation to
416 hypoxia is considered to be necessary for clinical pathogenesis because the conditions
417 *in vivo*, such as inside macrophages or granulomas, are hypoxic[38,45]. However, our strain
418 M001 entered log phase later than ATCC13950 under 5% oxygen. Our inability to
419 construct knockdown strains in M001 prevented us from clarifying its clinical
420 pathogenesis without preferential hypoxic adaptation. However, because we have shown
421 that most of the *M. intracellulare* strains with different genotypes showed preferential
422 adaptation to hypoxia in this study, our results largely reflect the clinical situation of the
423 etiological agents of MAC-PD. A possible strategy for identifying factors that confer
424 clinical pathogenesis will be to focus on the major clinical strains that show preferential
425 hypoxic adaption.

426 The data of validation of the universal essential or growth-defect associated
427 genes by the CRISPR-i system was overall acceptable in the clinically MAC-PD strains
428 whose knockdown strains could be constructed (Fig. 8a). However, we have
429 encountered the difficulties of validating the TnSeq-hit genes by CRISPR-i experiment,
430 especially accessory and strain-dependent essential or growth-defect-associated genes in
431 the MAC-PD strains other than M.i.198 or M003 (Fig. 8b, Supplementary Fig. 4). As a
432 possible reason, the low efficiency of the CRISPR-i system may obscure the increase in

433 gene essentiality suggested by the TnSeq data (Supplementary Fig. 5). The efficiency of
434 the suppression of gene expression by CRISPR-i in accessory and strain-dependent
435 essential or growth-defect-associated genes was lower in our *M. intracellulare* strains
436 than in Mtb[28]. In Mtb, the expression of *mmpL3*, a gene encoding a mycolic acid
437 transporter, is reported to be suppressed to 6% under 10 ng/ml anhydrotetracycline (aTc)
438 and by < 1% under 100 ng/ml aTc in the knockdown strains, compared to strains
439 expressing scrambled single guide RNAs (sgRNA)[28]. The gene expression levels were
440 suppressed in our knockdown strains by around 10%–40% under 50–200 ng/ml aTc
441 relative to the levels found in strains not expressing sgRNA (Supplementary Fig. 5). The
442 growth inhibition effect is theoretically dependent upon the degree to which gene
443 expression is suppressed. On the other hand, the inconsistent growth phenotypes of
444 knockdown strains of accessory and strain-dependent essential or growth-defect-
445 associated genes between MAC-PD strains implies some differences in the degree of
446 suppression of gene expression required to inhibit bacterial growth between genes as
447 well as between bacterial strains. Despite the issue of the lower efficiency of the
448 CRISPR-I system in *M. intracellulare* than in Mtb, this study has opened the avenue for
449 functional analysis of NTM that leads to the development of novel drugs that target
450 universal and accessory/strain-dependent essential metabolic pathways that has

451 significant impact on bacterial growth, especially by making use of M.i.198 and M003
452 as optimal NTM strains for gene manipulation.
453 As in the *glpX*-knockdown strains, *csd* knockdown caused growth suppression in
454 several MAC-PD strains. This type II Csd is involved in the biosynthesis of the iron–
455 sulfur clusters of the SUF machinery. Compared with the type I cysteine desulfurase
456 IscS, the SUF machinery is active under oxidative-stress and iron-limiting conditions[46].
457 Representatives of iron–sulfur cluster proteins include components of the electron-
458 transport system, such as NADH dehydrogenase I (Nuo) and succinate dehydrogenase
459 (Sdh), which are components of respiratory complexes I and II, respectively. Under
460 hypoxic conditions, the non-proton-translocating type II NADH dehydrogenase Ndh is
461 upregulated, and cytochrome *bd* oxidase (CydAB) and the proton-pumping type I
462 NADH dehydrogenase (Nuo) are downregulated[38]. In the reverse TCA cycle on the
463 same reaction pathway as Sdh, fumarate reductase (Fnr) is also an iron–sulfur cluster
464 protein that produces succinate, and is a proposed alternative electron acceptor under
465 hypoxic conditions[34,47]. The increased essentiality of the *csd* gene observed in the
466 clinical MAC-PD strains seems to reflect the switching of the electron-transport system
467 to less-energy-efficient respiration to support preferential hypoxic survival, including *in*
468 *vivo*.

469 We tried to use inhibitors of phosphoenolpyruvate carboxykinase to confirm the
470 increased essentiality of the *pckA* gene. However, we detected no positive effect because
471 millimolar 3-mercaptopicolinic acid is required to show the effect of inhibition, even in
472 eukaryotic cells, which have no cell wall[48]. Moreover, 3-alkyl-1,8-dibenzylxanthine[49]
473 also only effectively inhibits PckA in eukaryotic cells. However, PckA has been
474 proposed as a drug target for Mtb[50], so our TnSeq data seem to be consistent with
475 studies directed towards antimycobacterial drug discovery.
476 In summary, we have identified 131 universal essential and growth-defect-
477 associated genes that covers the genomic diversity of *M. intracellulare* strains
478 responsible for MAC-PD, which narrowed down the drug targets against MAC-PD.
479 Furthermore, we have demonstrated a preferential adaptation to hypoxia in clinical
480 NTM strains compared with the type strain in terms of the increased essentiality of
481 genes required for hypoxic growth, such as those encoding phosphoenolpyruvate
482 carboxykinase, the ESX-5 type VII secretion system, and cysteine desulfurase. These
483 genes were shown to have a significant impact on infection *in vivo* by increasing their
484 gene requirements. Our data highlight the importance of using clinical strains and
485 hypoxic conditions in experimental research, and provide fundamental resources for
486 developing novel drugs directed towards nontuberculous mycobacterial strains that

487 cause severe clinical diseases.

488

489 **Methods**

490 **Bacterial strains and phages used to prepare Tn mutants**

491 A total of nine strains were used in this study, including seven clinical strains isolated
492 from patients with MAC-PD in Japan (M.i.198, M.i.27, M018, M003, M019, M021,
493 and M001)[51], *M. intracellulare* genovar *paraintracellulare* type strain MOTT64 isolated
494 from MAC-PD in South Korea[52], and the *M. intracellulare* type strain ATCC13950 (Fig.
495 1). The Tn mutant libraries were constructed using glucose as a carbon source under
496 aerobic conditions according to the transduction method used for ATCC13950[9], except
497 that a higher concentration of kanamycin (100 μg/ml) was used to select the transposon
498 mutants than was used for ATCC13950 (25 μg/ml). In brief, a hundred milliliter of the
499 bacteria were cultured aerobically in 7H9/ADC broth until mid-log phase (optical
500 density at a wavelength of 600 nm [OD_{600}] of approximately 0.4–0.6). After harvesting
501 the bacteria, 10 mL of high-titer mycobacteriophage phAE180[53] was transduced into the
502 bacteria 1-day at 37°C for inserting Tn and plated on 7H10/OADC agar plates
503 containing kanamycin. After 2 or 3 week-cultivation at 37°C aerobically, the colonies
504 were harvested *en masse* and used as Tn mutant libraries. The kanamycin-resistant

505 colonies (> 1 × 10^5) were harvested and evenly resuspended in 7H9/ADC medium

506 containing 20% glycerol, aliquoted, and stored at −80 °C until further use.

507 **Next-generation sequencing and TnSeq analysis**

508 DNA libraries were prepared as reported previously[54]. The TnSeq libraries were

509 sequenced with the NextSeq 500 System, 150-bp single-end run (Illumina, San Diego,

510 CA, USA). The sequence reads were analyzed as previously described[9]. Gene

511 essentiality was calculated with resampling and HMM analyses using TRANSIT[11].

512 First, an HMM analysis was conducted to calculate the fluctuation of the number of Tn

513 insertion reads individually for each strain. Next, a resampling analysis was conducted

514 to calculate the difference of the number of Tn insertion reads between each clinical

515 strain and ATCC13950 (Supplementary Table 6). By comparing the data obtained by

516 HMM and resampling analyses, we summarized the difference of gene essentiality

517 between the clinical MAC-PD strains and ATCC13950. To compare the gene

518 essentiality of the clinical MAC-PD strains and ATCC13950, the annotation for the

519 clinical MAC-PD strains was adapted from that of ATCC13950 by adjusting the START

520 and END coordinates of each open reading frame (ORF) in the clinical MAC-PD strains

521 according to their alignment with the corresponding ORFs of ATCC13950. The function

522 of TnSeq-hit genes was categorized according to the Kyoto Encyclopedia of Genes and

523 Genomes (KEGG) database.

524 **Comparison of growth curves under aerobic and hypoxic conditions**

525 First, we precultured the bacteria in 7H9/ADC broth until the bacteria reached early log-
526 phase (OD_{600} approximately 0.1–0.3). Next, the bacterial cultures were diluted with new
527 7H9/ADC broth (final OD_{600} 0.003) for the aerobic and hypoxic growth assay. Bacterial
528 cells were grown statically in 96-well plates containing 250 μl of 7H9/ADC broth in
529 each well under aerobic conditions or 5% oxygen at 37 °C with humidification (APM-
530 30D incubator, Astec, Tokyo, Japan). The culture was sampled every 1–3 days. At
531 sampling, the culture was mixed by pipetting 50 times. An aliquot (4 μl) of the culture
532 and its diluents were streaked onto 7H10/OADC agar and the CFUs counted. The
533 growth curve was fitted to the logistic 4P model with the JMP software (SAS Institute
534 Inc., Cary, NC, USA) to calculate the inflection point (midpoint) and growth rate at
535 midpoint in the log growth phase. Entry into the log phase was evaluated from the
536 timing of the inflection point on the growth curve.

537 **Animals**

538 Female C57BL/6JJcl mice were purchased from CLEA Japan (Tokyo, Japan). Six-
539 week-old mice were used for the infection experiment (Supplementary Fig. 1). All the
540 mice were kept under specific-pathogen-free conditions in the animal facility of Niigata

541 University Graduate School of Medicine, according to the institutional guidelines for
542 animal experiments. The mice were housed (four per cage) under a 12-h/12-h light/dark
543 cycle. Food and water were available *ad libitum*. Kanamycin was added to the drinking
544 water to a final concentration of 100 μg/ml to maintain the mice's resistance to the Tn
545 mutant strains. Euthanasia was conducted with an intraperitoneal injection of a
546 combined anesthetic (15 μg of medetomidine, 80 μg of midazolam, and 100 μg of
547 butorphanol), followed by cervical dislocation.

548 **Mouse TnSeq experiment**

549 The protocol was based on our previous mouse lung infection experiment[51]. Twenty
550 mice each were used for the Tn mutant strains M.i.198 and M.i.27. The mice were
551 injected intratracheally with 3.25×10^8 and 5.93×10^7 CFUs of the Tn mutant strains,
552 respectively. The infected lungs were expected to be harvested from five mice at day 1,
553 week 4, week 8, and week 16 after infection. However, the lungs were harvested from
554 only four mice infected with the M.i.27 Tn mutant strains in week 8 because we
555 experienced difficulties with sampling, and the lungs were harvested from only three,
556 one, and two mice infected with M.i.198 Tn mutant strains in week 8, week 12, and
557 week 16, respectively, because morbidity was high in the mice infected with M.i.198.
558 The harvested lungs were homogenized in 4.5 ml of distilled water with the

559 gentleMACS™ Tissue Dissociator (Miltenyi Biotec, Bergish Gladbach, Germany) and

560 the homogenates were plated on Middlebrook 7H10–oleic acid ADC (7H10-OADC)

561 agar plates and cultured for 3 weeks. The colonies were harvested *en masse* for TnSeq.

562 **Gene set enrichment analysis**

563 To investigate the overlap of the gene sets required for growth in mouse lungs with

564 those required for hypoxic pellicle formation observed in ATCC13950 and those

565 showing increased gene essentiality observed in the clinical MAC-PD strains, a

566 statistical enrichment of gene sets was performed by GSEA 4.3.2[20]. Parameters set for

567 GSEA were as follows: permutations = 1,000, permutation type: gene_set, enrichment

568 statistic: weighted, metric for ranking genes: Signal2Noise, max size: 500, min size: 15.

569 **Construction and growth assay of knockdown strains**

570 Knockdown strains were constructed with the CRISPR-dCas9-mediated RNA

571 interference system, as reported previously[27]. Gene-specific 20-nt sequences were

572 selected as protospacers for incorporation into the sgRNAs (Supplementary Table 13).

573 pRH2502 (a vector expressing an inactivated version of the *cas9* DNA sequence) and

574 pRH2521 (an sgRNA-expressing vector whose expression is regulated by the TetR-

575 regulated smyc promotor P_{myc1}tetO) were introduced into the bacteria to obtain colonies

576 of the knockdown strains. For selection, 25 μg/ml kanamycin and 50 μg/ml hygromycin

577 were used for ATCC13950, and 100 μg/ml kanamycin and 50 μg/ml hygromycin were
578 used for the clinical strains. The growth assay of the knockdown strains was performed
579 in 7H9/ADC broth containing the above-mentioned concentrations of kanamycin and
580 hygromycin under aerobic conditions at 37 °C with humidification (APM-30D
581 incubator, Astec, Tokyo, Japan). During the assay, the cultures were supplemented with
582 anhydrotetracycline (aTc) to a final concentration of 50 ng/ml (as a concentration that is
583 not toxic to ATCC13950 and M.i.27) or 200 ng/ml (for the other clinical strains). aTc
584 was added repeatedly every 48 h to maintain the induction of dCas9 and sgRNAs in
585 experiments that extended beyond 48 h[27]. An aliquot (4 μl) of the culture and its diluents
586 were streaked onto 7H10/OADC agar plates containing kanamycin and hygromycin,
587 and the CFUs were counted. Growth inhibition was evaluated as the ratio of the CFUs
588 of knockdown strains compared with those of the vector control strains lacking the
589 guide RNA sequence. To confirm the downregulation of gene expression in the
590 knockdown strains, quantitative reverse transcription PCR (qRT-PCR) was performed.
591 Bacteria were cultured in 10 ml of Middlebrook 7H9 medium (Difco Laboratories,
592 Detroit, MI, USA) containing 0.2% glycerol, 0.1% Tween 80 (MP Biochemicals,
593 Illkrich, France), and 10% Middlebrook albumin–dextrose–catalase (7H9/ADC/Tween
594 80), kanamycin, and hygromycin until mid-log phase (OD_{600} approximately 0.4–0.6).

595 The cultures were supplemented with aTc every 48 h, as in the growth assay for the
596 knockdown strains. One day after the second addition of aTc, RNA was extracted by
597 bead-beating six times at 5000 rpm for 30 s with cooling (Micro Smash MS 100R Cell
598 Disruptor; Tomy Seiko, Tokyo, Japan) and cDNA was synthesized with the Direct-zol™
599 RNA Miniprep (Zymo Research, Orange, CA, USA) and ReverTra Ace qPCR RT
600 Master Mix with gDNA Remover (Toyobo, Osaka, Japan). qRT-PCR was performed
601 with the CFX Connect Real-time PCR Detection System (Bio-Rad, Hercules, CA,
602 USA), according to the manufacturer's instructions. The data were normalized to the
603 expression of *sigA*.

604 **Statistical analyses**

605 Pearson's correlation test was performed between the fitness costs ($\log_2$FC calculated by
606 the resampling assay), efficiency of knockdown (assessed by qRT-PCR) and growth
607 suppression in the knockdown strains. Statistical analyses of the growth curves were
608 performed using a 4-parameter logistic model (logistic 4P model), Wilcoxon two-
609 sample test, and a one-way analysis of variance (ANOVA) followed by Steel's multiple
610 comparisons test using the JMP software program (SAS Institute Inc., Cary, NC, USA).
611 Data are presented as the mean ± SD. Statistical significance was set as *P* values less
612 than 0.05.

613

614 [References]

615 1. Adjemian, J., Olivier, K.N., Seitz, A.E., Holland, S.M. & Prevots, D.R.
616 Prevalence of nontuberculous mycobacterial lung disease in U.S. Medicare
617 beneficiaries. *Am J Respir Crit Care Med* **185**, 881-886 (2012).

618 2. Namkoong, H. *et al.* Epidemiology of pulmonary nontuberculous mycobacterial
619 disease, Japan. *Emerg Infect Dis* **22**, 1116-1117 (2016).

620 3. Daley, C.L. *et al.* Treatment of nontuberculous mycobacterial pulmonary
621 disease: an official ATS/ERS/ESCMID/IDSA clinical practice guideline. *Eur*
622 *Respir J* **56**, 2000535 (2020).

623 4. Uchiya, K.I. *et al.* Comparative genome analyses of *Mycobacterium avium*
624 reveal genomic features of its subspecies and strains that cause progression of
625 pulmonary disease. *Sci Rep* **7**, 39750 (2017).

626 5. Tateishi, Y. *et al.* Comparative genomic analysis of *Mycobacterium*
627 *intracellulare*: implications for clinical taxonomic classification in pulmonary
628 *Mycobacterium avium-intracellulare* complex disease. *BMC Microbiol* **21**, 103
629 (2021).

630 6. Tortoli, E. *et al.* Genome-based taxonomic revision detects a number of
631 synonymous taxa in the genus *Mycobacterium*. *Infect Genet Evol* **75**, 103983
632 (2019).

633 7. van Opijnen, T. & Camilli, A. Transposon insertion sequencing: a new tool for
634 systems-level analysis of microorganisms. *Nat Rev Microbiol* **11**, 435-442
635 (2013).
636 8. Carey, A.F. *et al.* TnSeq of *Mycobacterium tuberculosis* clinical isolates reveals
637 strain-specific antibiotic liabilities. *PLoS Pathog* **14**, e1006939 (2018).
638 9. Tateishi, Y. *et al.* Genome-wide identification of essential genes in
639 *Mycobacterium intracellulare* by transposon sequencing - Implication for
640 metabolic remodeling. *Sci Rep* **10**, 5449 (2020).
641 10. Cuttino, J.T. & Mc, C.A. Pure granulomatous nocardiosis, a new fungus disease
642 distinguished by intracellular parasitism; a description of a new disease in man
643 due to a hitherto undescribed organism, *Nocardia intracellularis*, n. sp.,
644 including a study of the biologic and pathogenic properties of this species. *Am J*
645 *Pathol* **25**, 1-47 (1949).
646 11. DeJesus, M.A., Ambadipudi, C., Baker, R., Sassetti, C. & Ioerger, T.R.
647 TRANSIT--A Software Tool for Himar1 TnSeq Analysis. *PLoS Comput Biol* **11**,
648 e1004401 (2015).
649 12. Krieger, I.V. *et al.* Structure-guided discovery of phenyl-diketo acids as potent
650 inhibitors of *M. tuberculosis* malate synthase. *Chem Biol* **19**, 1556-1567 (2012).

651 13. Rosconi, F. *et al.* A bacterial pan-genome makes gene essentiality strain-
652 dependent and evolvable. *Nat Microbiol* **7**, 1580–1592 (2022).
653 14. Coll, F. *et al.* Genome-wide analysis of multi- and extensively drug-resistant
654 *Mycobacterium tuberculosis*. *Nat Genet* **50**, 307-316 (2018).
655 15. Nguyen, H.T., Wolff, K.A., Cartabuke, R.H., Ogwang, S. & Nguyen, L. A
656 lipoprotein modulates activity of the MtrAB two-component system to provide
657 intrinsic multidrug resistance, cytokinetic control and cell wall homeostasis in
658 *Mycobacterium*. *Mol Microbiol* **76**, 348-364 (2010).
659 16. Li, S. *et al.* CRISPRi chemical genetics and comparative genomics identify
660 genes mediating drug potency in *Mycobacterium tuberculosis*. *Nat Microbiol.* **7**,
661 766–779 (2022).
662 17. Kirschner, R.A., Jr., Parker, B.C. & Falkinham, J.O., 3rd. Epidemiology of
663 infection by nontuberculous mycobacteria. *Mycobacterium avium,*
664 *Mycobacterium intracellulare,* and *Mycobacterium scrofulaceum* in acid, brown-
665 water swamps of the southeastern United States and their association with
666 environmental variables. *Am Rev Respir Dis* **145**, 271-275 (1992).
667 18. Werner, E. *et al.* Stratified growth in *Pseudomonas aeruginosa* biofilms. *Appl*
668 *Environ Microbiol* **70**, 6188-6196 (2004).

669 19. Via, L.E. *et al.* Tuberculous granulomas are hypoxic in guinea pigs, rabbits, and
670 nonhuman primates. *Infect Immun* **76**, 2333-2340 (2008).
671 20. Subramanian, A. *et al.* Gene set enrichment analysis: A knowledge-based
672 approach for interpreting genome-wide expression profiles. *Proc Natl Acad Sci*
673 *U S A* **102,** 15545–15550 (2005).
674 21. Kryzywinska, E., Bhatnagar, S., Sweet, L., Chatterjee, D. & Schorey, J.S.
675 *Mycobacterium avium* 104 deleted of the methyltransferase D gene by allelic
676 replacement lacks serotype-specific glycopeptidolipids and shows attenuated
677 virulence in mice. *Mol Microbiol* **56**, 1262-1273 (2005).
678 22. Irani, V.R., Lee, S.-H., Eckstein, T.M., Inamine, J.M., Belisle, J.T. & Maslow,
679 J.N. Utilization of a ts-sacB selection system for the generation of a
680 *Mycobacterium avium* serovar-8 specific glycopeptidolipid allelic exchange
681 mutant. A*nnals Clin Microbiol Antimicrob* **3**, 18 **(**2004).
682 23. Marklund, B.I., Speert, D.P. & Stokes, R.W. Gene replacement through
683 homologous recombination in *Mycobacterium intracellulare*. *J Bacteriol* **177**,
684 6100-6105 (1995).
685 24. Marklund, B.I., Mahenthiralingam, E. & Stokes, R.W. Site-directed mutagenesis
686 and virulence assessment of the *katG* gene of *Mycobacterium intracellulare*. *Mol*

687 *Microbiol* **29**, 999-1008 (1998).

688 25. Mahenthiralingam, E., Marklund, B.I., Brooks, L.A., Smith, D.A., Bancroft, G.J.
689 & Stokes, R.W. Site-directed mutagenesis of the 19-kilodalton lipoprotein
690 antigen reveals No essential role for the protein in the growth and virulence of
691 *Mycobacterium intracellulare*. *Infect Immun*. **66**, 3626-3634 (1998).

692 26. Hinds, J. *et al.* Enhanced gene replacement in mycobacteria. *Microbiology* **145**,
693 519-527 (1999).

694 27. Singh, A.K. *et al.* Investigating essential gene function in *Mycobacterium*
695 *tuberculosis* using an efficient CRISPR interference system. *Nucleic Acids Res*
696 **44**, e143 (2016).

697 28. McNeil, M.B. & Cook, G.M. Utilization of CRISPR interference to validate
698 MmpL3 as a drug target in *Mycobacterium tuberculosis*. *Antimicrob Agents*
699 *Chemother* **63,** e00629-19 (2019).

700 29. Yang, T. *et al.* Pan-genomic study of *Mycobacterium tuberculosis* reflecting the
701 primary/secondary genes, generality/individuality, and the interconversion
702 through copy number variations. *Front Microbiol* **9**, 1886 (2018).

703 30. Nick, J.A. *et al.* Host and pathogen response to bacteriophage engineered against
704 *Mycobacterium abscessus* lung infection. *Cell* **185**, 1860-1874.e12 (2022).

705 31. Eoh, H. *et al.* Metabolic anticipation in *Mycobacterium tuberculosis*. *Nat*
706 *Microbiol* **2**, 17084 (2017).
707 32. Lim, J. *et al.* Phosphoenolpyruvate depletion mediates both growth arrest and
708 drug tolerance of *Mycobacterium tuberculosis* in hypoxia. *Proc Natl Acad Sci U*
709 *S A* **118,** e2105800118 (2021).
710 33. Marrero, J., Rhee, K.Y., Schnappinger, D., Pethe, K. & Ehrt, S. Gluconeogenic
711 carbon flow of tricarboxylic acid cycle intermediates is critical for
712 *Mycobacterium tuberculosis* to establish and maintain infection. *Proc Natl Acad*
713 *Sci U S A* **107**, 9819-9824 (2010).
714 34. Watanabe, S. *et al.* Fumarate reductase activity maintains an energized
715 membrane in anaerobic *Mycobacterium tuberculosis*. *PLoS Pathog* **7**, e1002287
716 (2011).
717 35. Gouzy, A., Healy, C., Black, K.A., Rhee, K.Y. & Ehrt, S. Growth of
718 *Mycobacterium tuberculosis* at acidic pH depends on lipid assimilation and is
719 accompanied by reduced GAPDH activity. *Proc Natl Acad Sci U S A* **118,**
720 e2024571118 (2021).
721 36. Quinonez, C.G. *et al.* The role of fatty acid metabolism in drug tolerance of
722 *Mycobacterium tuberculosis*. *mBio* **13**, e0355921 (2022).

723 37. Pandey, A.K. & Sassetti, C.M. Mycobacterial persistence requires the utilization
724 of host cholesterol. *Proc Natl Acad Sci U S A* **105**, 4376-4380 (2008).
725 38. Prosser, G. *et al.* The bacillary and macrophage response to hypoxia in
726 tuberculosis and the consequences for T cell antigen recognition. *Microbes*
727 *Infect* **19**, 177-192 (2017).
728 39. Dragset, M.S. *et al.* Global assessment of *Mycobacterium avium* subsp.
729 *hominissuis* genetic requirement for growth and virulence. *mSystems* **4,** e00402-
730 19 (2019).
731 40. Ates, L.S. *et al.* Essential role of the ESX-5 secretion system in outer membrane
732 permeability of pathogenic mycobacteria. *PLoS Genet* **11**, e1005190 (2015).
733 41. Ates, L.S. *et al.* The ESX-5 system of pathogenic mycobacteria is nvolved in
734 capsule integrity and virulence through its substrate PPE10. *PLoS Pathog* **12**,
735 e1005696 (2016).
736 42. Savitskaya, A. *et al.* C-terminal intrinsically disordered region-dependent
737 organization of the mycobacterial genome by a histonelike protein. *Sci Rep* 8, 1–
738 15 (2018).
739 43. Enany, S. *et al.* Mycobacterial DNA-binding protein 1 is critical for long term
740 survival of Mycobacterium smegmatis and simultaneously coordinates cellular

741 functions. *Sci Rep* 7, 1–11 (2017).

742 44. Shaban, A.K. *et al.* Mycobacterial DNA-binding protein 1 is critical for BCG
743 survival in stressful environments and simultaneously regulates gene expression.
744 *Sci Rep* 13, 14157 (2023).

745 45. Rustad, T.R., Sherrid, A.M., Minch, K.J. & Sherman, D.R. Hypoxia: a window
746 into *Mycobacterium tuberculosis* latency. *Cell Microbiol* **11**, 1151-1159 (2009).

747 46. Takahashi, Y. & Tokumoto, U. A third bacterial system for the assembly of iron-
748 sulfur clusters with homologs in archaea and plastids. *J Biol Chem* **277**, 28380-
749 28383 (2002).

750 47. Cecchini, G., Schröder, I., Gunsalus, R.P. & Maklashina, E. Succinate
751 dehydrogenase and fumarate reductase from *Escherichia coli*. *Biochim Biophys*
752 *Acta* **1553**, 140-57 (2002).

753 48. Brearley, M.C., Daniel, Z., Loughna, P.T., Parr, T. & Brameld, J.M. The
754 phosphoenolpyruvate carboxykinase (PEPCK) inhibitor, 3-mercaptopicolinic
755 acid (3-MPA), induces myogenic differentiation in C2C12 cells. *Sci Rep* **10**,
756 22177 (2020).

757 49. Montal, E.D. *et al.* Inhibition of phosphoenolpyruvate carboxykinase blocks
758 lactate utilization and impairs tumor growth in colorectal cancer. *Cancer Metab*

759 **7**, 8 (2019).

760 50. McLeod, M.J., Krismanich, A.P., Assoud, A., Dmitrienko, G.I. & Holyoak, T.
761 Characterization of 3-[(carboxymethyl)thio]picolinic acid: a novel inhibitor of
762 phosphoenolpyruvate carboxykinase. *Biochemistry* **58**, 3918-3926 (2019).

763 51. Tateishi, Y. *et al.* Virulence of *Mycobacterium intracellulare* clinical strains in a
764 mouse model of lung infection - role of neutrophilic inflammation in disease
765 severity. *BMC Microbiol* **23**, 94 (2023).

766 52. Kim, B.J. *et al.* Complete genome sequence of *Mycobacterium intracellulare*
767 clinical strain MOTT-64, belonging to the INT1 genotype. *J Bacteriol* **194**, 3268
768 (2012).

769 53. Kriakov, J., Lee, S. & Jacobs, W.R., Jr. Identification of a regulated alkaline
770 phosphatase, a cell surface-associated lipoprotein, in *Mycobacterium smegmatis*.
771 *J Bacteriol* **185**, 4983-4991 (2003).

772 54. Minato, Y. *et al.* Genomewide assessment of *Mycobacterium tuberculosis*
773 conditionally essential metabolic pathways. *mSystems* **4,** e00070-19 (2019).

774 55. Shannon, P. *et al.* Cytoscape: a software environment for integrated models of
775 biomolecular interaction networks. *Genome Res* **13**, 2498-2504 (2003).

776

Acknowledgments

The authors thank Dr. Torin Weisbrod and Dr. William R. Jacobs, Jr. (Albert Einstein College of Medicine, Bronx, NY, USA) for kindly providing mycobacterial phage phAE180, and Dr. Norikazu Hara and Dr. Takeshi Ikeuchi (Department of Molecular Genetics, Bioresource Science, Brain Center for Bioresources, Brain Research Institute, Niigata University) for next-generation sequencing with the NextSeq 500 System. This work was supported by Grants-in-Aid for Scientific Research (grant numbers 20KK0216, 21K19637, and 22H03115 to Yoshitaka Tateishi) from the Ministry of Health, Labour, and Welfare, of Japan This work was also supported by grants from the Japanese Ministry of Education, Culture, Sports, Science, and Technology, the Ministry of Health, and the Research Program on Emerging Infectious Disease from the Japan Agency for Medical Research and Development (23fk0108673h0501).

Author contributions

Y.T. conceived, designed and performed the experiments. Y.O., A.N., and S.M. contributed reagents or materials. Y. Morishige., Y. Minato, and A.D.B. contributed analytical tools. Y. Morishige., Y. Minato, A.D.B., and S.M. provided critical suggestions throughout the preparation of the manuscript. Y.T. wrote the manuscript. All authors read

795 and approved the final manuscript.

796

797 **Availability of data and materials**

798 The datasets used or analyzed in this study are available from the corresponding author

799 upon reasonable request.

800

801 **Declarations**

802 **Ethics approval and consent to participate**

803 All experimental protocols were approved by the Institutional Review Board of Niigata

804 University (approval numbers: 2019-0020 for the use of human tissue samples and

805 SA00506 for experiments on live vertebrates). All experiments on humans and human

806 samples were conducted in accordance with relevant guidelines and regulations. Informed

807 consent was obtained from all patients. All experiments on animals were conducted in

808 accordance with the relevant guidelines and regulations, and the study complied with the

809 ARRIVE guidelines.

810 **Consent for publication**

811 According to the protocols approved by the Institutional Review Board of Niigata

812 University mentioned above, consent for publication was obtained from the patients

enrolled in this study.

Competing interests

The authors declare that they have no competing interests.

817 **Fig. 1 Phylogenetic tree of the *M. intracellulare* strains and strategy of the**
818 **experiment in this study. a** Phylogenetic tree of the *M. intracellulare* strains used in this
819 study. The tree was generated based on average nucleotide identity (ANI) with the
820 neighbor-joining method. TMI: typical *M. intracellulare*; MP-MIP: *M.*
821 *paraintracellulare–M. indicus pranii*. **b** Strategy of the experimental procedure.
822
823 **Fig. 2 Identification of the essential and growth-defect-associated genes across all**
824 **nine *M. intracellulare* strains used in this study. a** Functional categories of 131 genes
825 identified as universal essential or growth-defect-associated with an HMM analysis. The
826 genes were categorized according to the Kyoto Encyclopedia of Genes and Genomes
827 (KEGG) database. **b** Universal essential or growth-defect-associated genes corresponding
828 to the genes of existing antituberculous drug targets. **c** The number of the essential or
829 growth-defect-associated genes in the accessory genome, and the number of strain-
830 dependent essential or growth-defect-associated genes in the core genome.
831
832 **Fig. 3 Detection of genes showing increased or reduced gene essentiality in the**
833 **clinical *M. intracellulare* strains.** Left panel shows the genes identified as having fewer
834 Tn insertion reads than the type strain ATCC13950. The fold changes in the number of

835 Tn insertion reads calculated by a resampling analysis are represented by the color scale.
836 Red squares indicate genes required for hypoxic pellicle formation in ATCC13950[9].
837 *Genes identified with a combination of resampling and HMM analyses. †Genes
838 identified only with resampling analysis. Right panel shows the genes identified as having
839 more Tn insertion reads than type strain ATCC13950. NH: no homolog with ATCC13950,
840 NS: no significant increase in Tn insertion reads by a resampling analysis (adjusted $P <$
841 0.05).
842
843 **Fig. 4 Overview of the differences in gene essentiality between the clinical *M.*
844 *intracellulare* strains and ATCC13950, drawn with Cytoscape[55].** Each central node
845 represents the functional category of genes, assigned with a KEGG pathway analysis.
846 Each peripheral node represents the genes showing significant changes in the number of
847 Tn insertion reads. The size of each node represents the number of strains identified. Each
848 edge represents a strain identified as showing significant changes in the number of Tn
849 insertion reads. The thickness of each edge represents the adjusted *P* value. The color
850 scale of each edge represents the fold change in the number of Tn insertion reads
851 calculated by a resampling analysis. The graphical organization was referenced to the
852 previous publication by Carey, *et al*[8].

853

854 **Fig. 5 Preferential gene requirements for gluconeogenesis in the clinical *M.***

855 ***intracellulare* strains inferred from the TnSeq results. a** Carbohydrate pathway

856 showing the changes in Tn insertion reads. Genes identified with the resampling

857 analysis are framed by squares. The essentiality of gluconeogenesis-related genes (*pckA,*

858 *glpX*) was higher and that of glycolysis-related genes (*aceE, lpdC*) was lower in the

859 clinical *M. intracellulare* strains compared with those in ATCC13950. **b** Data on gene

860 essentiality calculated with a resampling analysis in the clinical *M. intracellulare* strains

861 compared with ATCC13950. Red indicates a reduction in Tn insertion reads in the

862 clinical *M. intracellulare* strains. Blue indicates an increase of Tn insertion reads in the

863 clinical *M. intracellulare* strains. Asterisks indicate statistical significance of $\log_2$ fold

864 changes ($\log_2$FCs). The graphical organization was referenced to the previous

865 publication by Carey, *et al*[8].

866

867 **Fig. 6 Significance of increased gene essentiality profiles *in vitro* on the**

868 **pathogenesis of mouse lung infection. a** Consistency between the genes required for

869 infection in mouse lungs and the 175 genes required for hypoxic pellicle formation in

870 ATCC13950. **b** Changes in the requirements for genes with increased essentiality

871 observed in the clinical *M. intracellulare* strains after the infection of mouse lungs.

872 Highlighted genes are also required for hypoxic pellicle formation by ATCC13950.

873 Gene essentiality of the strain itself: gene essentiality compared with that of

874 ATCC13950. Gene requirements in mouse lungs: changes in the gene requirements in

875 the infected mouse lungs compared with those before infection. Gene set enrichment

876 analysis: The genes listed as core enrichment are shown as "Yes" and the genes not

877 listed as core enrichment are shown as "No."

878

879 **Fig. 7 Comparison of the timing of entry into logarithmic growth and logarithmic**

880 **growth rate by the clinical *M. intracellulare* strains and ATCC13950. a** Time at the

881 inflection point (midpoint) on the sigmoid growth curve. *significantly earlier than an

882 aerobic culture of ATCC13950; #significantly earlier than a hypoxic culture of

883 ATCC13950; †significantly later than an aerobic culture of ATCC13950; ‡significantly

884 later than a hypoxic culture of ATCC13950. **b** Growth rate at midpoint of the growth

885 curve in each strain. #significantly slower than a hypoxic culture of ATCC13950;

886 †significantly slower than an aerobic culture of the corresponding strain; ‡significantly

887 faster than an aerobic culture of ATCC13950. Open bars: aerobic; closed bars: 5% O_2.

888 Data are shown as the means ± SD of triplicate experiments. Data from one experiment

889 representative of three independent experiments ($N = 3$) are shown.

890

891 **Fig. 8 Validation of the inhibition of bacterial growth caused by the suppression of**

892 **the expression of TnSeq-hit genes using the CRISPR-i system.** Open bar: day 3;

893 closed bar: day 7. **a** Comparative growth rates of the knockdown strains relative to those

894 of the vector control strains in the representative universal essential or growth-defect-

895 associated genes: *glcB, inhA*, *gyrB* and *embB*. **b** Comparative growth rates of the

896 knockdown strains relative to those of the vector control strains in the representative

897 accessory and strain-dependent essential or growth-defect-associated genes: *pckA*, *glpX*,

898 *csd* and ESX-5 type VII secretion components. Data are shown as the means ± SD of

899 triplicate experiments. Data from one experiment representative of two independent

900 experiments ($N = 2$) are shown.

901

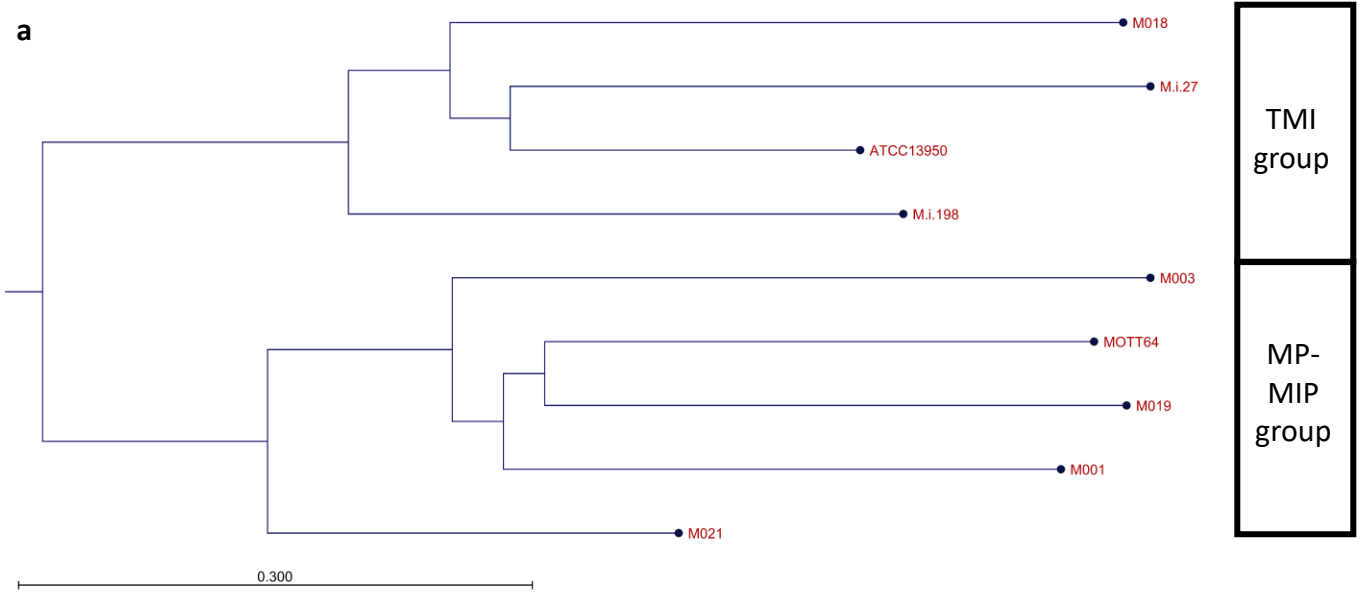

b

Prepare Tn mutant libraries

Clinical MAC-PD strains			Reference strain
M.i.198	M001	M021	ATCC13950
M.i.27	M003	MOTT64	
M018	M019		

TnSeq

Detect universal and accessory/strain-dependent essential or growth- defect-associated genes among clinical MAC-PD strains and ATCC13950 by an Hidden Markov Model (HMM) analysis

Compare gene essentiality between clinical MAC-PD strains and ATCC13950 by HMM and resampling analyses (The annotation for the clinical strains has been adapted from the ATCC13950.)

Detect genes showing significantly reduced or increased Tn insertion reads

Detect genes required for mouse lung infection and evaluate the impact of genes showing increased gene essentiality in clinical MAC-PD strains compared to ATCC13950 on mouse lung infection

Validate the gene essentiality by CRISPR-i for the representative universal and accessory/strain-dependent shared essential or growth- defect-associated genes and for the genes showing significantly reduced Tn insertion reads in clinical MAC-PD strains compared to ATCC13950

Fig. 1

a

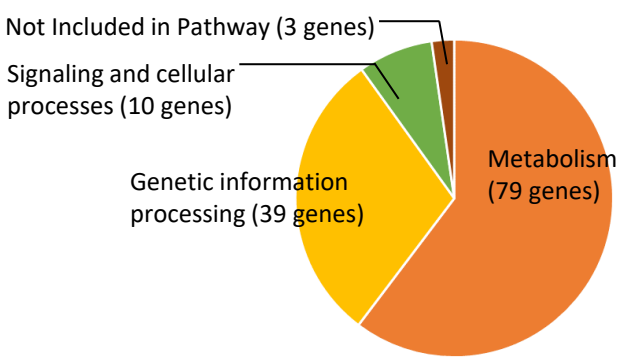

Metabolism: glyoxylate, purine/pyrimidine, amino acid, lipid, arabinogalactan/peptidoglycan, porphyrin

Genetic information processing: DNA replication, transcription, amino acid tRNA ligases, ribosomal proteins, general Sec proteins

Signaling and cellular processes: ABC transporter, type VII secretion system, iron-sulfur cluster assembly

Not Included in Pathway: hypothetical proteins

b

Gene locus	gene	function	target drug
OCU_RS25020, OCU_RS25025	*gyrB, gyrA*	DNA topoisomerase subunit B, intein-containing DNA gyrase subunit A	fluoroquinolones
OCU_RS26150	*embB*	arabinosyltransferase	ethambutol
OCU_RS40185	*inhA*	enoyl[acyl-carrier-protein] reductase FabI	isoniazid/ethionamid
OCU_RS45570	*alr*	alanine racemase	cycloserine
OCU_RS46225	*rpoC*	DNA-directed RNA polymerase subunit beta'	rifampicin
OCU_RS38100	*glcB*	malate synthase G	malate synthase inhibitors
OCU_RS32840, OCU_RS32845, OCU_RS32850	*atpA, atpG, atpB*	F_0F_1 ATP synthase subunit alpha, gamma, beta	bedaquiline

c

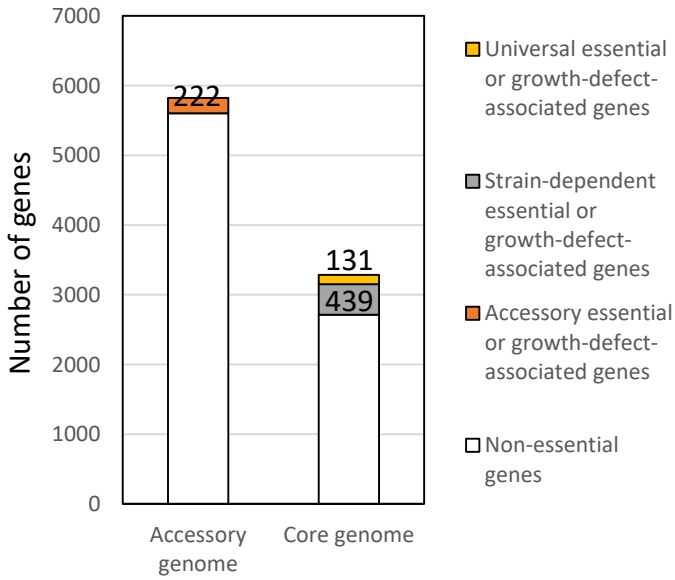

Fig. 2

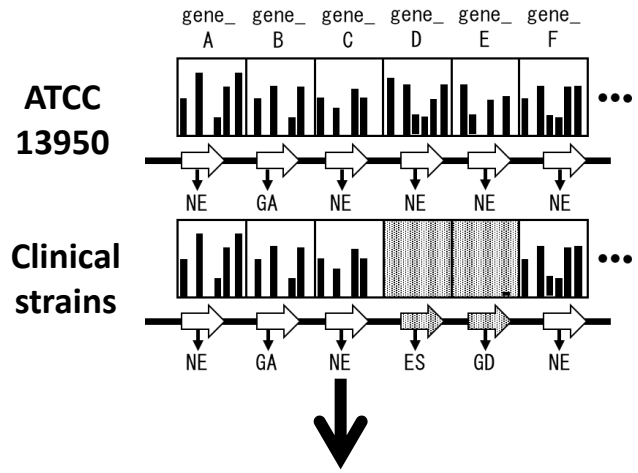

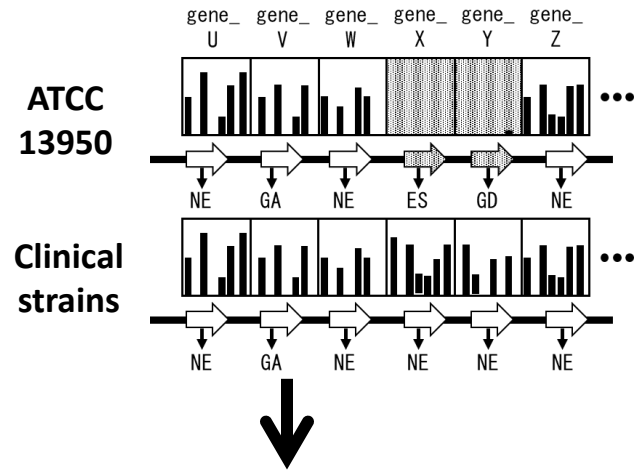

Tn decrease in clinical strains

A total of 121 genes were detected as significantly reduced Tn in clinical MAC-PD strains compared to ATCC13950. Of those, 9 genes were commonly hit in 3 to 5 clinical strains.

Tn increase in clinical strains

A total of 162 genes were detected as significantly increased Tn insertion compared to ATCC13950. Of those, 12 genes were commonly hit in more than 7 clinical MAC-PD strains.

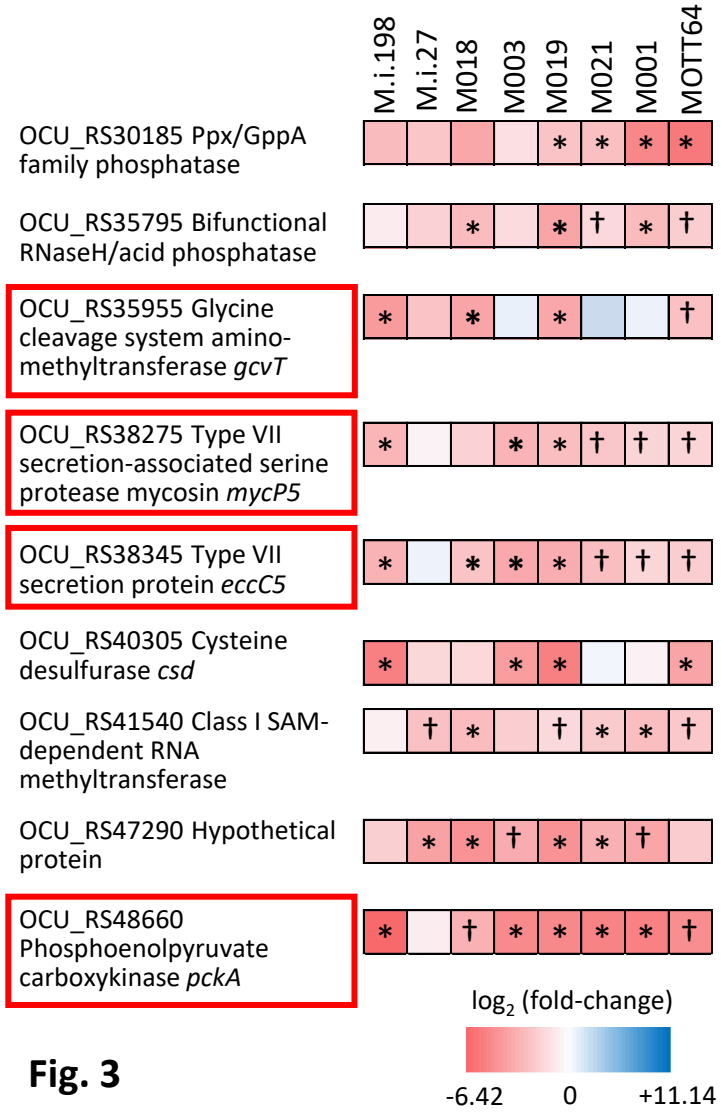

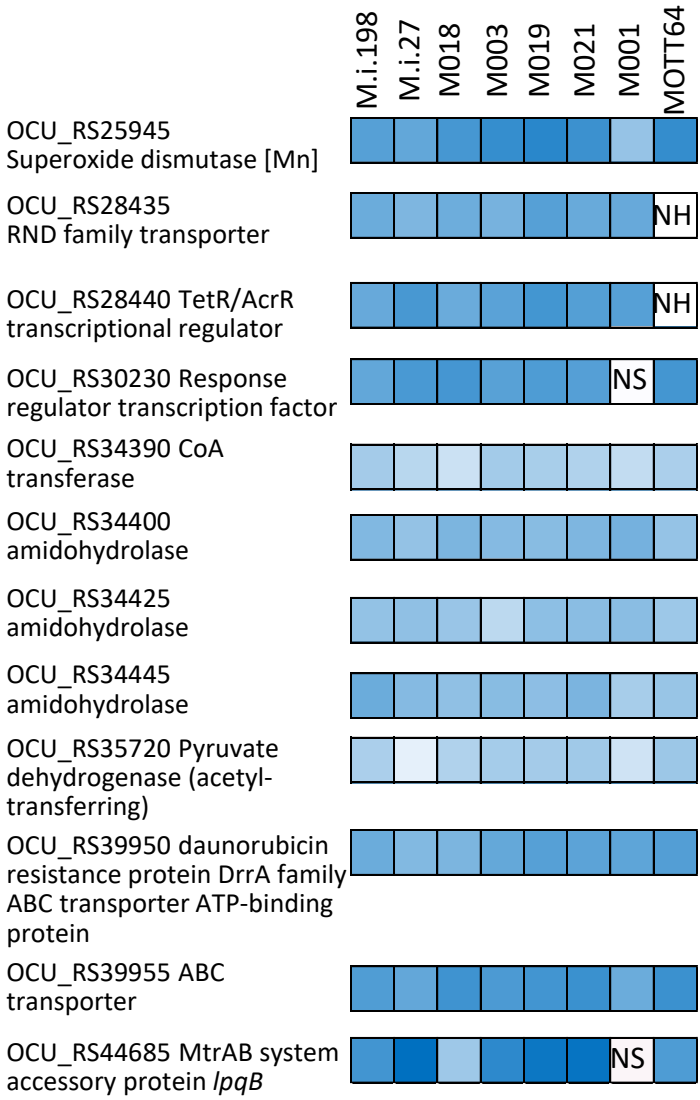

Fig. 3

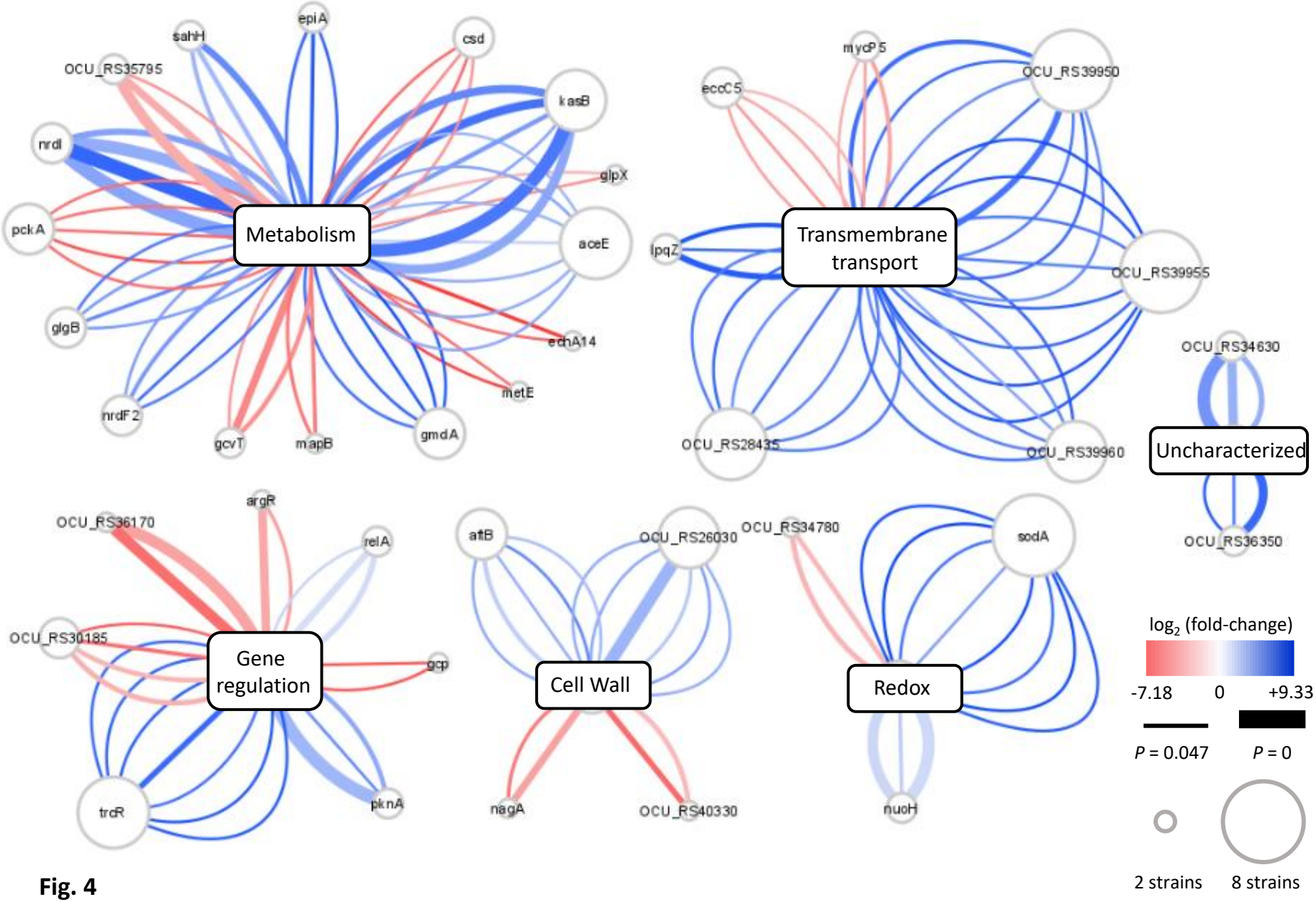
Metabolism
epiA
sahH
csd
OCU_RS35795
kasB
nrdI
glpX
pckA
aceE
glgB
echA14
metE
nrdF2
gcvT
mapB
gmdA
Transmembrane transport
mycP5
OCU_RS39950
eccC5
lpqZ
OCU_RS39955
OCU_RS28435
OCU_RS39960
Uncharacterized
OCU_RS34630
OCU_RS36350
Gene regulation
argR
OCU_RS36170
relA
OCU_RS30185
gcp
trcR
pknA
Cell Wall
aftB
OCU_RS26030
nagA
OCU_RS40330
Redox
OCU_RS34780
sodA
nuoH
log2 (fold-change)
-7.18
0
+9.33
P = 0.047
P = 0
2 strains
8 strains

Fig. 4

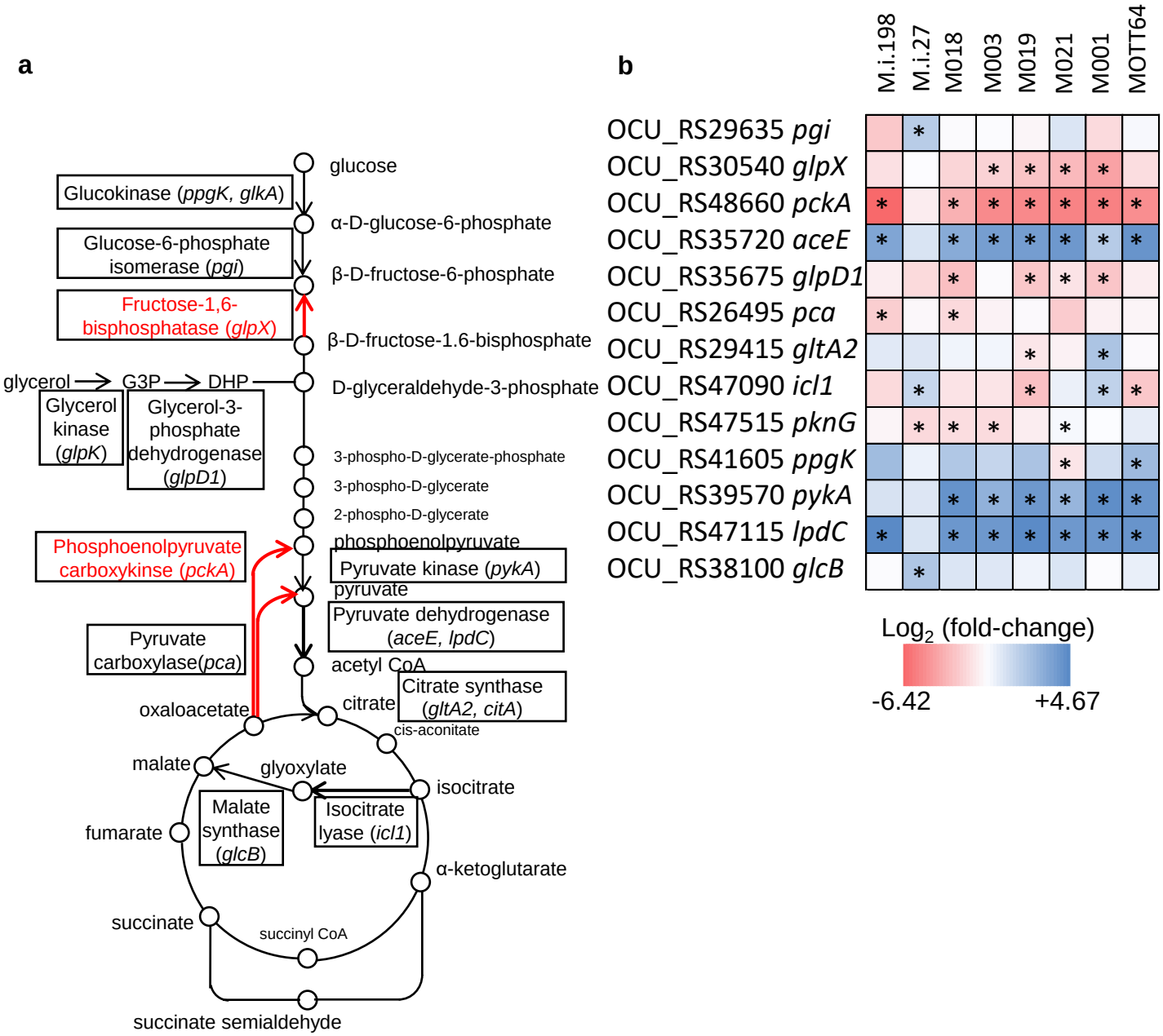
a
glucose
Glucokinase (ppgK, glkA)
α-D-glucose-6-phosphate
Glucose-6-phosphate isomerase (pgi)
β-D-fructose-6-phosphate
Fructose-1,6-bisphosphatase (glpX)
β-D-fructose-1.6-bisphosphate
glycerol
G3P
DHP
D-glyceraldehyde-3-phosphate
Glycerol kinase (glpK)
Glycerol-3-phosphate dehydrogenase (glpD1)
3-phospho-D-glycerate-phosphate
3-phospho-D-glycerate
2-phospho-D-glycerate
phosphoenolpyruvate
Phosphoenolpyruvate carboxykinse (pckA)
Pyruvate kinase (pykA)
pyruvate
Pyruvate dehydrogenase (aceE, lpdC)
Pyruvate carboxylase(pca)
acetyl CoA
Citrate synthase (gltA2, citA)
oxaloacetate
citrate
cis-aconitate
malate
glyoxylate
isocitrate
Malate synthase (glcB)
Isocitrate lyase (icl1)
fumarate
α-ketoglutarate
succinate
succinyl CoA
succinate semialdehyde
b
M.i.198
M.i.27
M018
M003
M019
M021
M001
MOTT64
OCU_RS29635 pgi
OCU_RS30540 glpX
OCU_RS48660 pckA
OCU_RS35720 aceE
OCU_RS35675 glpD1
OCU_RS26495 pca
OCU_RS29415 gltA2
OCU_RS47090 icl1
OCU_RS47515 pknG
OCU_RS41605 ppgK
OCU_RS39570 pykA
OCU_RS47115 lpdC
OCU_RS38100 glcB
Log2 (fold-change)
-6.42
+4.67

Fig 5.

a

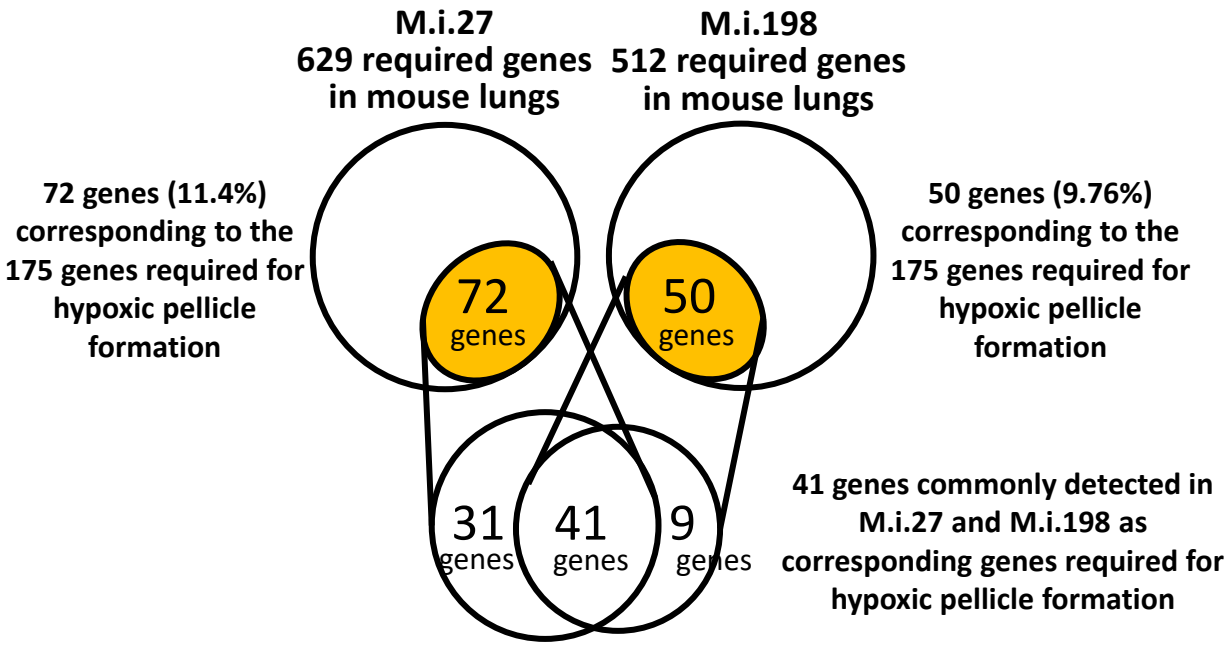

b

Locus_tag	Gene annotation	M.i.27 Gene essentia-lity of strain itself	M.i.27 Gene require-ments in mouse lungs	M.i.27 Gene set enrichi-ment analysis	M.i.198 Gene essentia-lity of strain itself	M.i.198 Gene require-ments in mouse lungs	M.i.198 Gene set enrichi-ment analysis
OCU_RS48660	Phoshoenolpyruvate carboxykinase PckA	NC	UP	Yes	UP	NC	No
OCU_RS30540	Fructose-1,6-bisphosphatase GlpX	NC	UP	Yes	NC	NC	Yes
OCU_RS40305	Cysteine desulfurase Csd	NC	UP	Yes	UP	NC	No
OCU_RS38345	TypeVII secretion protein EccC5	NC	UP	Yes	UP	NC	Yes
OCU_RS38275	TypeVII serine protease MycP5	NC	UP	Yes	UP	NC	No
OCU_RS35955	Glycine cleavage system aminomethyltransferase GcvT	NC	UP	Yes	UP	NC	Yes
OCU_RS30185	Ppx/GppA family phosphatase	NC	NC	Yes	NC	NC	Yes
OCU_RS35795	Bifunctional RNaseH/acid phosphatase	NC	NC	No	NC	NC	Yes
OCU_RS41540	Class I SAM-dependent RNA methyltransferase	UP	NC	No	NC	UP	Yes
OCU_RS47290	Hypothetical protein	UP	NC	Yes	NC	NC	Yes

Fig. 6

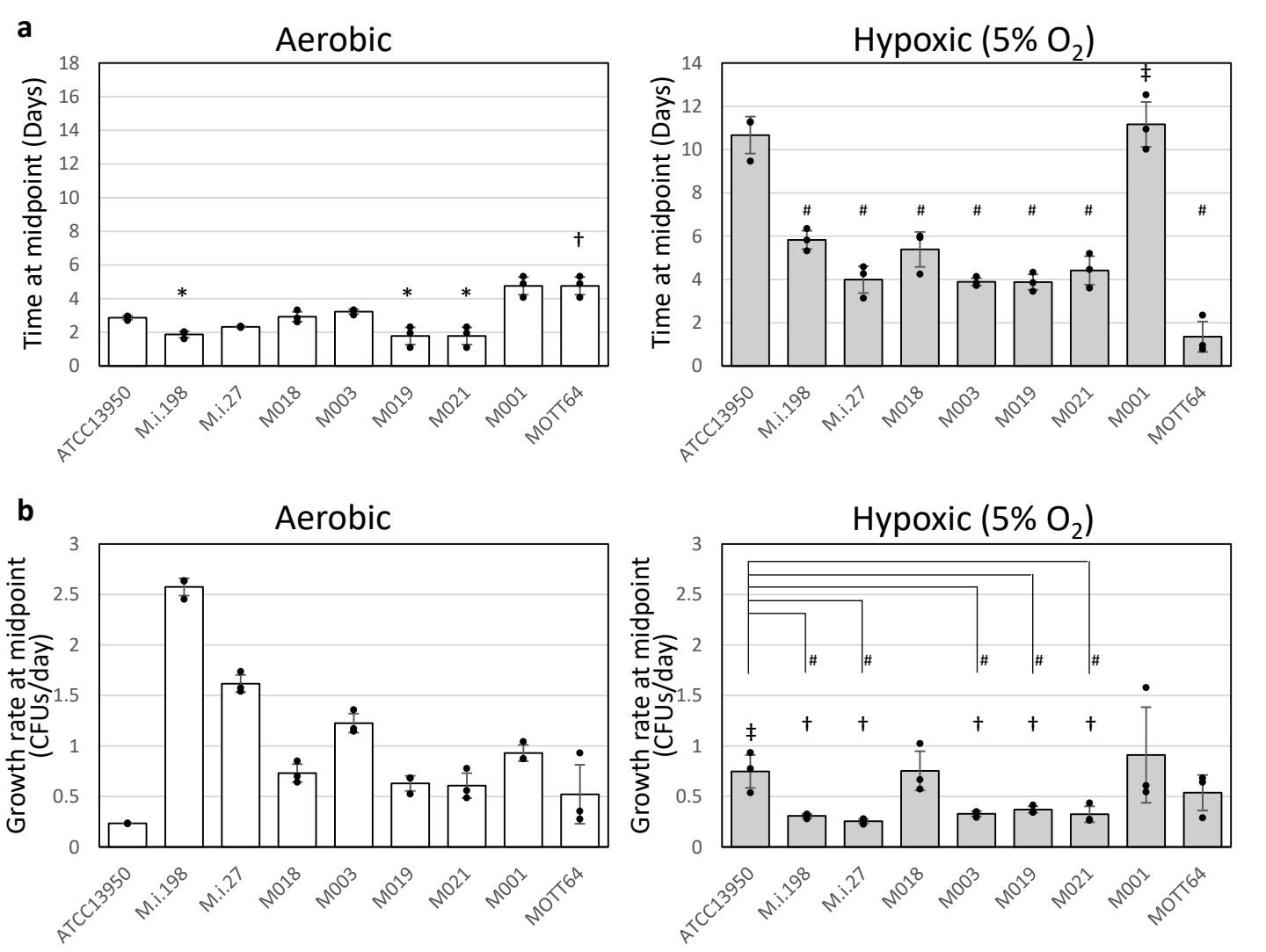
a
Aerobic
Hypoxic (5% O2)
Time at midpoint (Days)
b
Growth rate at midpoint (CFUs/day)
ATCC13950
M.i.198
M.i.27
M018
M003
M019
M021
M001
MOTT64

Fig. 7

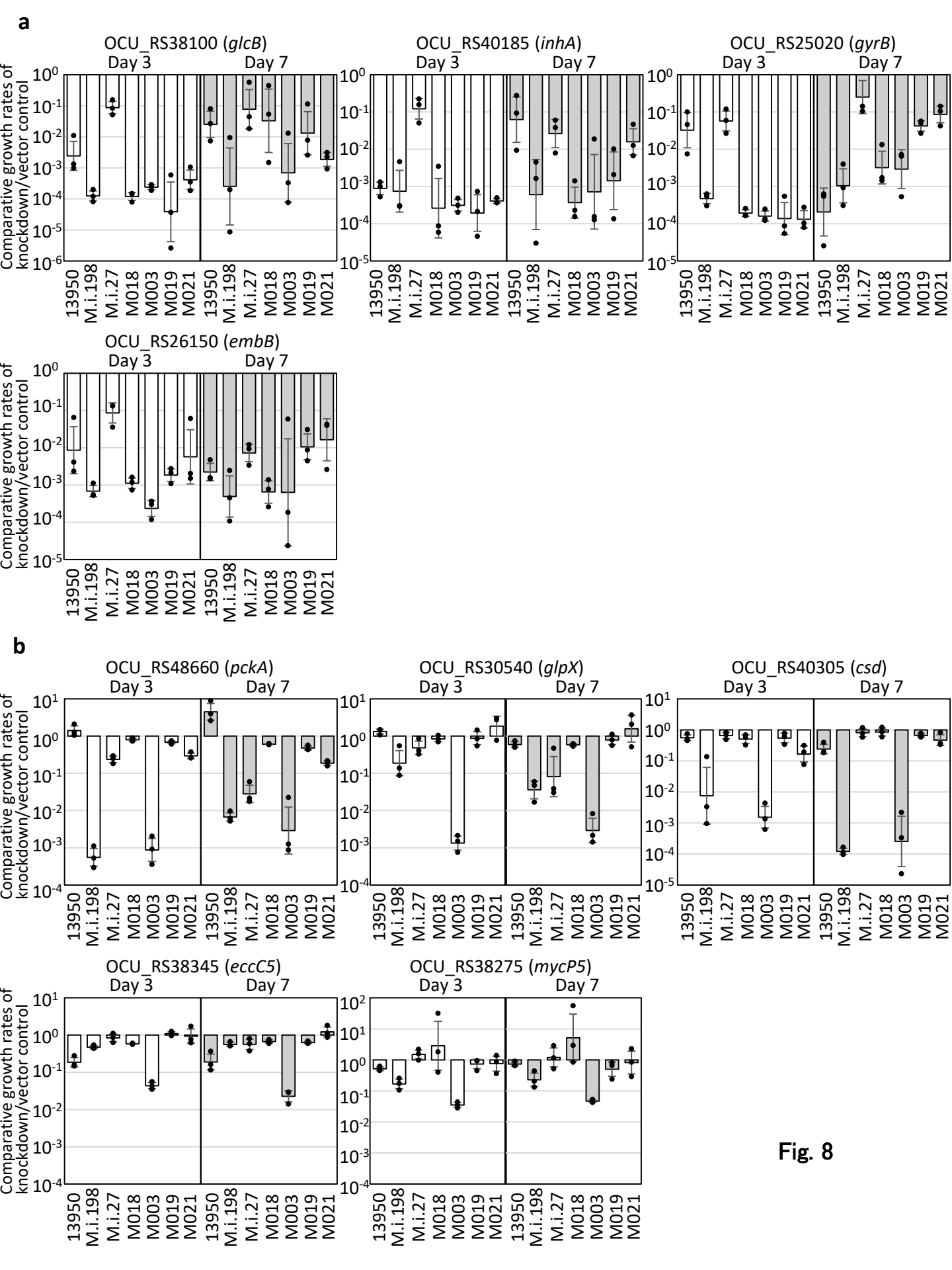
a
OCU_RS38100 (glcB)
OCU_RS40185 (inhA)
OCU_RS25020 (gyrB)
OCU_RS26150 (embB)
Day 3
Day 7
Comparative growth rates of knockdown/vector control
13950
M.i.198
M.i.27
M018
M003
M019
M021
b
OCU_RS48660 (pckA)
OCU_RS30540 (glpX)
OCU_RS40305 (csd)
OCU_RS38345 (eccC5)
OCU_RS38275 (mycP5)

Fig. 8